

NATIONAL AERONAUTICS AND SPACE ADMINISTRATION

Space Programs Summary No. 37-40, Volume VI

for the period May 1, 1966 to June 30, 1966

Space Exploration Programs and Space Sciences

GPO PRICE \$ _____

CFSTI PRICE(S) \$ _____

Hard copy (HC) 2.50

Microfiche (MF) .75

11 853 July 65

jpl

JET PROPULSION LABORATORY
CALIFORNIA INSTITUTE OF TECHNOLOGY
PASADENA, CALIFORNIA

FACILITY FORM 602

N66 38506

(ACCESSION NUMBER)

120

(PAGES)

CR-78552

(NASA CR OR TMX OR AD NUMBER)

(THRU)

1

(CODE)

31

(CATEGORY)

July 31, 1966

NATIONAL AERONAUTICS AND SPACE ADMINISTRATION

Space Programs Summary No. 37-40, Volume VI

for the period May 1, 1966 to June 30, 1966

Space Exploration Programs and Space Sciences

JET PROPULSION LABORATORY
CALIFORNIA INSTITUTE OF TECHNOLOGY
PASADENA, CALIFORNIA

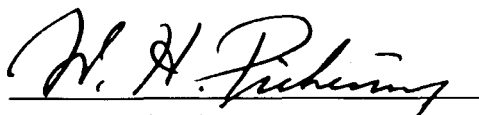
July 31, 1966

Preface

The *Space Programs Summary* is a six-volume, bimonthly publication that documents the current project activities and supporting research and advanced development efforts conducted or managed by JPL for the NASA space exploration programs. The titles of all volumes of the *Space Programs Summary* are:

- Vol. I. The Lunar Program (Confidential)
- Vol. II. The Planetary-Interplanetary Program (Confidential)
- Vol. III. The Deep Space Network (Unclassified)
- Vol. IV. Supporting Research and Advanced Development (Unclassified)
- Vol. V. Supporting Research and Advanced Development (Confidential)
- Vol. VI. Space Exploration Programs and Space Sciences (Unclassified)

The *Space Programs Summary*, Vol. VI consists of an unclassified digest of appropriate material from Vols. I, II, and III; an original presentation of technical supporting activities, including engineering development of environmental-test facilities, and quality assurance and reliability; and a reprint of the space science instrumentation studies of Vols. I and II. This instrumentation work is conducted by the JPL Space Sciences Division and also by individuals of various colleges, universities, and other organizations. All such projects are supported by the Laboratory and are concerned with the development of instruments for use in the NASA space flight programs.



W. H. Pickering, Director
Jet Propulsion Laboratory

Space Programs Summary No. 37-40, Volume VI

Copyright © 1966, Jet Propulsion Laboratory, California Institute of Technology
Prepared under Contract No. NAS 7-100, National Aeronautics & Space Administration

Contents

LUNAR PROGRAM

I. <i>Surveyor</i> Project	1
A. Introduction	1
B. <i>Surveyor I</i> Preflight, Flight and Postflight Operations	1
C. Systems Testing	8
D. Space Flight Operations	9
E. Electronics	10
F. Electrical Power Source	11
G. Propulsion	11
H. Payload and Scientific Mechanisms	15

PLANETARY-INTERPLANETARY PROGRAM

II. <i>Mariner 1967</i> Project	17
A. Introduction	17
B. Systems	18
III. <i>Mariner Mars 1969</i> Project	21
A. Introduction	21
IV. <i>Voyager</i> Project	23
A. Introduction	23

DEEP SPACE NETWORK

V. Introduction	25
VI. Facilities and Development	27
VII. Operational Activities	29
A. Station Preparation	29
B. Flight Project Support	30
C. Experimental Activities	30

SPACE SCIENCES

VIII. Lunar and Planetary Instruments	
A. <i>Surveyor</i> Single-Axis Seismometer Development	33

Contents (Cont'd)

IX. Space Instruments	40
A. <i>Mariner</i> Mars Magnetometer Configuration	40
B. <i>Mariner</i> Venus 67 Trapped Radiation Detectors	40
C. A New Method for Recording Video Signals on Magnetic Tape	42
X. Space Instrument Systems	45
A. <i>Mariner</i> Venus 67 Data Automation System	45
B. <i>Mariner</i> Venus 67 Data Automation System Format	47
XI. Lunar and Planetary Sciences	49
A. <i>Mariner</i> Venus 67 Dual-Frequency Radio Occultation Experiment	49
References	52
XII. <i>Mariner</i> Space Sciences	53
A. <i>Mariner</i> Venus 67 Encounter Sequence	53

SUPPORTING ACTIVITIES

XIII. Environmental Test Facilities	55
A. <i>Surveyor</i> and <i>Mariner</i> Venus 67 Solar Panel Thermal Radiation Fixture	55

LUNAR PROGRAM

I. *Surveyor* Project

A. Introduction

Surveyor I, the first of seven Model A-21 flight spacecraft, was launched from Cape Kennedy, Florida, at 14:41:00.990 GMT on May 30, 1966, and soft-landed on the Moon at 06:17:37 GMT on June 2, 1966. By June 14, when lunar sunset occurred, approximately 100,000 commands had been received by the spacecraft, and 10,338 pictures of the spacecraft and its immediate vicinity had been transmitted.

The Model A-21 flight spacecraft are designed to span the gap between the *Ranger* Project and Project *Apollo* by making soft-landings on the Moon to extend our knowledge of lunar conditions and determine the suitability of sites for proposed *Apollo* spacecraft landings. The engineering payload includes elements of redundancy, diagnostic telemetry, touchdown instrumentation, and survey TV.

Hughes Aircraft Company, Space Systems Division, is under contract to fabricate the Model A-21 spacecraft. The launch vehicle, a combination *Atlas/Centaur*, is provided by General Dynamics/Convair. Control, command,

and tracking functions for the *Surveyor* missions are performed by the JPL Deep Space Network and Mission Operations System.

The second *Surveyor* spacecraft launch is presently scheduled for the third quarter of 1966.

B. *Surveyor I* Preflight, Flight, and Postflight Operations

1. SC-1 (First Flight Spacecraft) Preflight Testing

Preparations at the Eastern Test Range for the joint flight-acceptance composite test (J-FACT) and pressure decay tests were completed April 14, and the SC-1 spacecraft was encapsulated the following day. After a systems readiness test, the SC-1 was transported to the launch pad and mated to its *Atlas/Centaur 10* launch vehicle on April 17. Tests in preparation for the J-FACT were performed, and compatibility tests of the spacecraft and the Deep Space Instrumentation Facility were

then begun on April 19. Three countdowns were conducted during the J-FACT on April 26: a test exercise, an *Atlas* problem situation, and a simulated liftoff.

After the J-FACT, two launch-readiness reviews were held, and the spacecraft was transported to the explosive safe facility for special tests. On May 4, rework, performance verification test preparations, and launch vehicle flight preparations were accomplished at the spacecraft checkout facility. A meeting was held on May 6 to review the performance of, and the problems resulting from, the J-FACT. None of the problems was serious, and the launch schedule was not affected.

The performance verification test begun May 8 was completed May 13. Propellant loading and final cleanup were performed at the propellant loading building, and weight and balance checks were conducted at the flight assembly building. Another launch-readiness review was held on May 24. A performance verification pre-encapsulation test and a launch vehicle composite readiness test were completed May 25, and the spacecraft was checked for flight readiness and encapsulated the following day. All planned tests and checks of the launch vehicle, launch complex, weather, range, spacecraft, and operations were reported as being successfully completed at the final mission-readiness meeting held 24 hr prior to launch.

2. Surveyor I (SC-1) Mission Operations

a. Launch through spacecraft separation from Centaur stage. Surveyor I was launched on a direct-ascent lunar-intercept trajectory at 14:41:00.990 GMT on May 30, 1966. The launch azimuth was 102.285 deg from true north. The boost phase was normal, with injection occurring at 14:52:30 GMT.

Just prior to spacecraft separation, the *Centaur* stage issued the preprogrammed commands for accomplishing spacecraft operations required for the post-separation phase, namely: extending landing gears, extending omniantennas, and turning on transmitter high power. Normal response to the first and third commands was verified by telemetry received by downrange ships, but, in response to the second command, only omnidirectional antenna B extension was confirmed (i. e., telemetry indicated that omnidirectional antenna A had not extended).

Spacecraft separation occurred at 14:53:38 GMT. Each of the springs released by explosively actuated latch pins operated normally. The uniform extension of the springs and the vehicle residual motion imparted an

approximately 0.34-deg/sec vector-sum turn rate to the spacecraft, well below the allowed 3-deg/sec value. The actual measured times of the major flight events between liftoff and spacecraft separation agreed very closely with preflight estimates. The only significant difference was the burn time of the *Centaur* engines, which was approximately 5 sec longer than expected. This was probably the result of the actual thrust being lower than the value used in preflight simulations.

b. Sun acquisition and establishment of DSIF two-way lock. After separation, the spacecraft executed its automatic sequences as designed. By use of cold-gas jets, the flight-control subsystem nulled out the rotational rates imparted by the separation springs and initiated a roll, yaw sequence to acquire the Sun. After a negative roll of approximately 100.5 deg and a positive yaw of 86 deg, acquisition and lock-on to the Sun by the spacecraft Sun sensors were completed at 15:00:34 GMT. Concurrently with this sequence, the automatic solar panel deployment sequence took place, being completed at 15:03:20 GMT. These operations were confirmed in real time by telemetry received by downrange ships.

At approximately 24 min after launch, *Surveyor I* became visible to the Johannesburg Deep Space Station (DSS), and initial acquisition procedures for establishing the communications and tracking link between the spacecraft and the DSS were initiated. Less than 4 min later, at 15:08:41 GMT, two-way lock was established.

The first ground-controlled spacecraft sequence, which was initiated at 15:20:42 GMT, consisted of commands for turning off equipment no longer required, seating the solar panel and roll axis locking pins securely, increasing the telemetry bit rate to 1100 bits/sec, and initially interrogating all telemetry commutator modes so that the spacecraft's over-all condition could be assessed. All spacecraft responses to commands were normal. Since telemetry still indicated that omnidirectional antenna A was not extended, a command was sent to extend the antenna, but no response was obtained.

c. Premidcourse coast, including Canopus acquisition. The spacecraft continued to coast with its pitch and yaw attitude controlled to track the Sun and with its roll axis held inertially fixed. A roll sequence was initiated to obtain data for a star map and to acquire Canopus so that the roll attitude could be fixed to a precise position from which the midcourse maneuver could be initiated. Star intensity signals from seven stars in addition to Canopus were identified during the first revolution, with Canopus

being observed and identified after 220 deg of roll. Since the Canopus intensity signal was above the upper threshold of the lock-on range, a lock-on signal was not obtained as the Canopus sensor swept past Canopus. As the vehicle continued to roll, computations were made of the time for sending the proper command to achieve manual lock-on to Canopus (when the vehicle had rolled to the proper position). A command was sent at the computed time, and manual lock-on was achieved at 19:13:20 GMT. *Surveyor I* then continued to coast as before, but with its roll attitude controlled so that the Canopus sensor remained locked onto Canopus.

At 5 hr after separation of the spacecraft from the *Centaur* stage, the minimum required separation distance between the two vehicles was 336 km. The actual value was approximately 1,054 km. The *Centaur* continues to travel in a highly elliptical Earth orbit with an apogee of approximately 237,000 nm and a period of approximately 12 days.

During this coast phase lasting until execution of the midcourse maneuver, continuous telemetry was received from *Surveyor I* at 1100 bits/sec until approximately 11 hr after launch and at 550 bits/sec thereafter. Three engineering interrogations (including two scheduled for transmitter high power) and a 3-hr check of the drift of the three gyros were performed during this period of low-power transmitter operation. All subsystems were performing satisfactorily.

d. Midcourse maneuver. All midcourse maneuver operations were performed in a normal manner. With the spacecraft visible to and controlled by the Pioneer DSS, the spacecraft was commanded to perform a negative roll of 86.5 deg at 06:20:23 GMT and a negative yaw of 57.9 deg at 06:34:14 GMT on May 31. With the vehicle's thrusting direction then positioned properly, the midcourse thrust was applied by igniting the vernier engines and controlling their thrust to achieve a constant spacecraft acceleration of 0.1 g for 20.8 sec. Analog recorder data verified that the thrust duration was correct; the actual time was 20.75 sec, a value well within the accuracy of the recorder.

A short-duration transient occurred on the Canopus sensor error signal 75 sec after the vernier propulsion system pressurization squib was actuated. The timing was such that this transient was very likely caused by a particle released by the squib which passed through the Canopus sensor field of view. No effect on the mission resulted.

Following the midcourse thrusting, the reverse maneuvers (positive yaw of 57.9 deg and positive roll of 86.5 deg) were performed successfully, with the Sun and Canopus sensors being illuminated properly. This confirmed that the gyros had retained their inertial reference during the vernier engine shutdown; therefore, a postmidcourse star verification was not necessary.

The following table demonstrates the accuracy of the midcourse maneuver. In terms of miss, the spacecraft injection errors would have resulted in only a 264-mile miss from the target area. As a result of the midcourse maneuver, the actual miss was less than 9 miles.

Target point	Latitude, deg S	Longitude, deg W
Initial aiming point (prelaunch)	3.25	43.83
Premidcourse landing point (if no midcourse maneuver were made)	11.43	54.25
Revised aiming point (point for which the midcourse maneuver was computed)	2.33	43.83
Actual landing point	2.411	43.36

e. Postmidcourse coast. Throughout this phase (which lasted until the initiation of the terminal descent maneuvers), the telemetry rate was 550 bits/sec. Five gyro-drift measurements and ten engineering interrogations were made. The drift of all gyros was below the specified upper limit. The temperature data channels not being sampled continuously indicated normal performance during the interrogations.

Power-mode cycling checks were made to help predict the percentage of the electrical load that would be supplied by each of the spacecraft batteries (main and auxiliary) during the terminal descent phase, when both batteries would be connected directly to the bus. To ensure that the auxiliary battery would be at the desired temperature $>60^{\circ}\text{F}$ at the time of terminal descent, it was decided to use both batteries to supply power immediately after the checks, with the auxiliary battery supplying most of the load to increase its rate of temperature rise from 1 to 2°F/hr to 3°F/hr .

f. Terminal descent. The terminal descent sequence was initiated with the turn-on of the high-power transmitter and the performance of the last engineering interrogation at 05:20:18 GMT on June 2. The telemetry

rate was changed to 1100 bit/sec at 05:21:27 GMT. A positive 89.3-deg roll maneuver and a positive 59.9-deg yaw maneuver were performed to orient the retrorocket engine thrust direction properly, and a positive 94.1-deg roll maneuver was then performed to position the omni antennas for optimum telecommunications performance during the retrorocket and vernier descent sequences.

The altitude marking radar turned on and was enabled and, except for two commands transmitted to the spacecraft (turn-on of touchdown strain gage data and establishment of optimum sampling rate for flight-control telemetry data), the remaining operations were performed automatically by the spacecraft. The altitude marking radar initiated the automatic descent sequence,

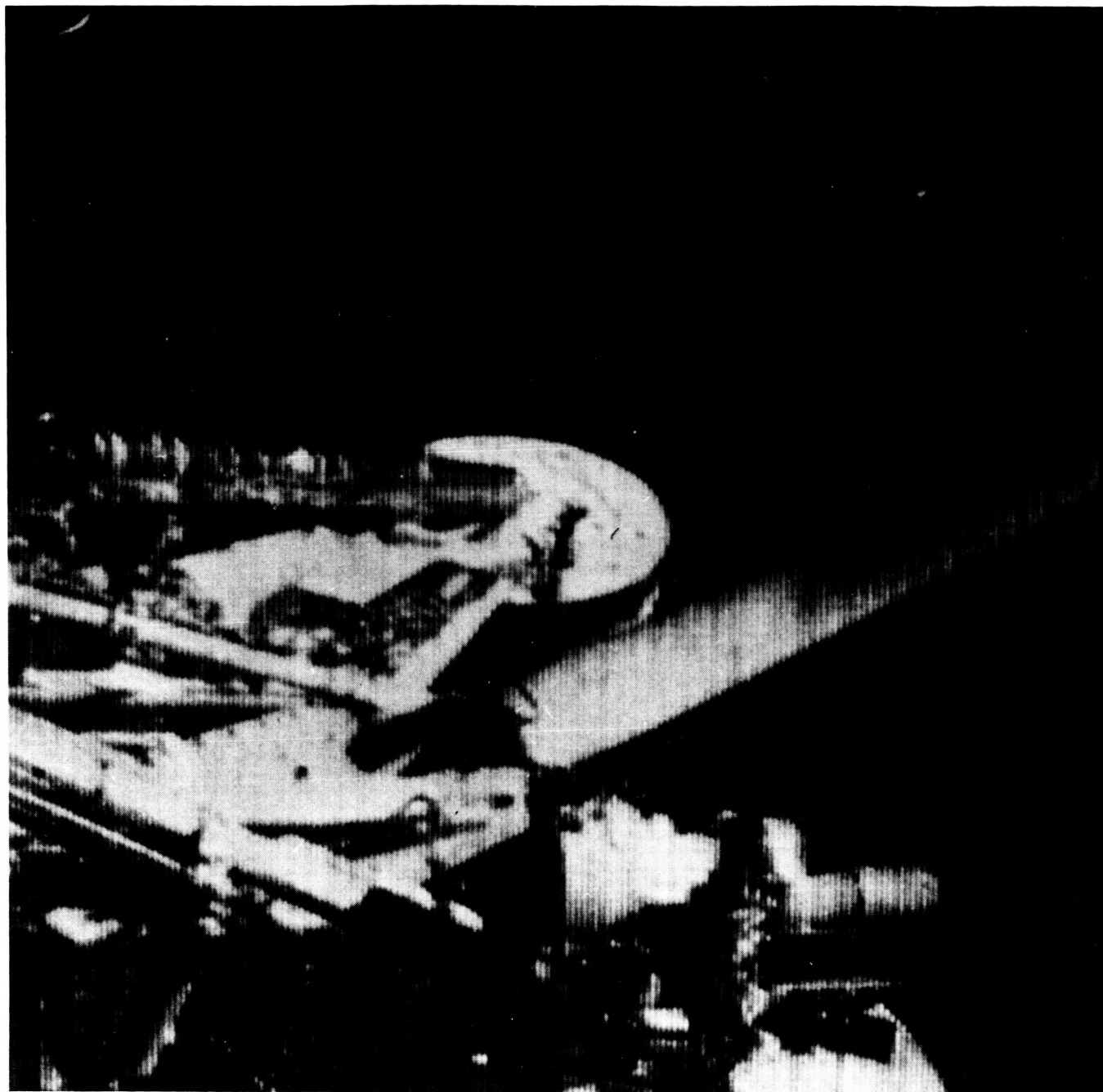


Fig. 1. First picture transmitted from *Surveyor 1* at 35 min after touchdown (200-line scan)

which included the following: vernier ignition, retro-rocket ignition, radar altimeter and doppler velocity sensor turn-on, retrorocket burnout and separation, enabling of doppler control, 1000-ft mark, 10-ft/sec mark, and 14-ft mark. "Quick-look" analysis of the telemetry indicated that touchdown occurred between 1 and 2 sec after the 14-ft mark at 06:17:37 GMT on June 2. (This,

the time the telemetry was received at the JPL Space Flight Operations Facility, includes the transit time from the spacecraft to the ground, the processing delay, and the commutation delay; thus, the time of touchdown could be in error by 0.5 sec.) As stated previously, the landing occurred at 2.36-deg south latitude and 43.36-deg west longitude, within 9 miles of the aiming point. The

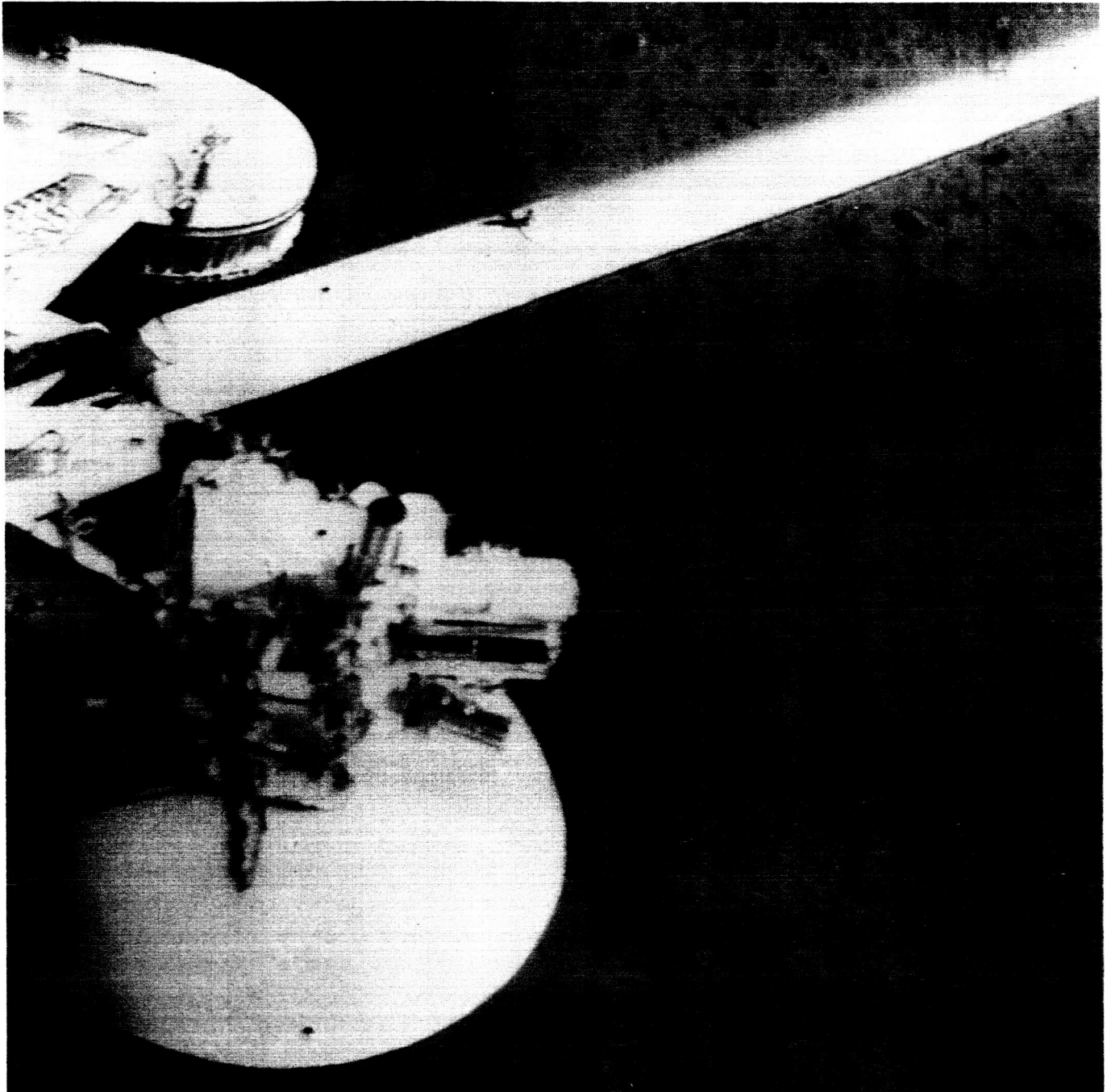


Fig. 2. Picture showing Surveyor 1 footpad and imprint created by impact (600-line scan)

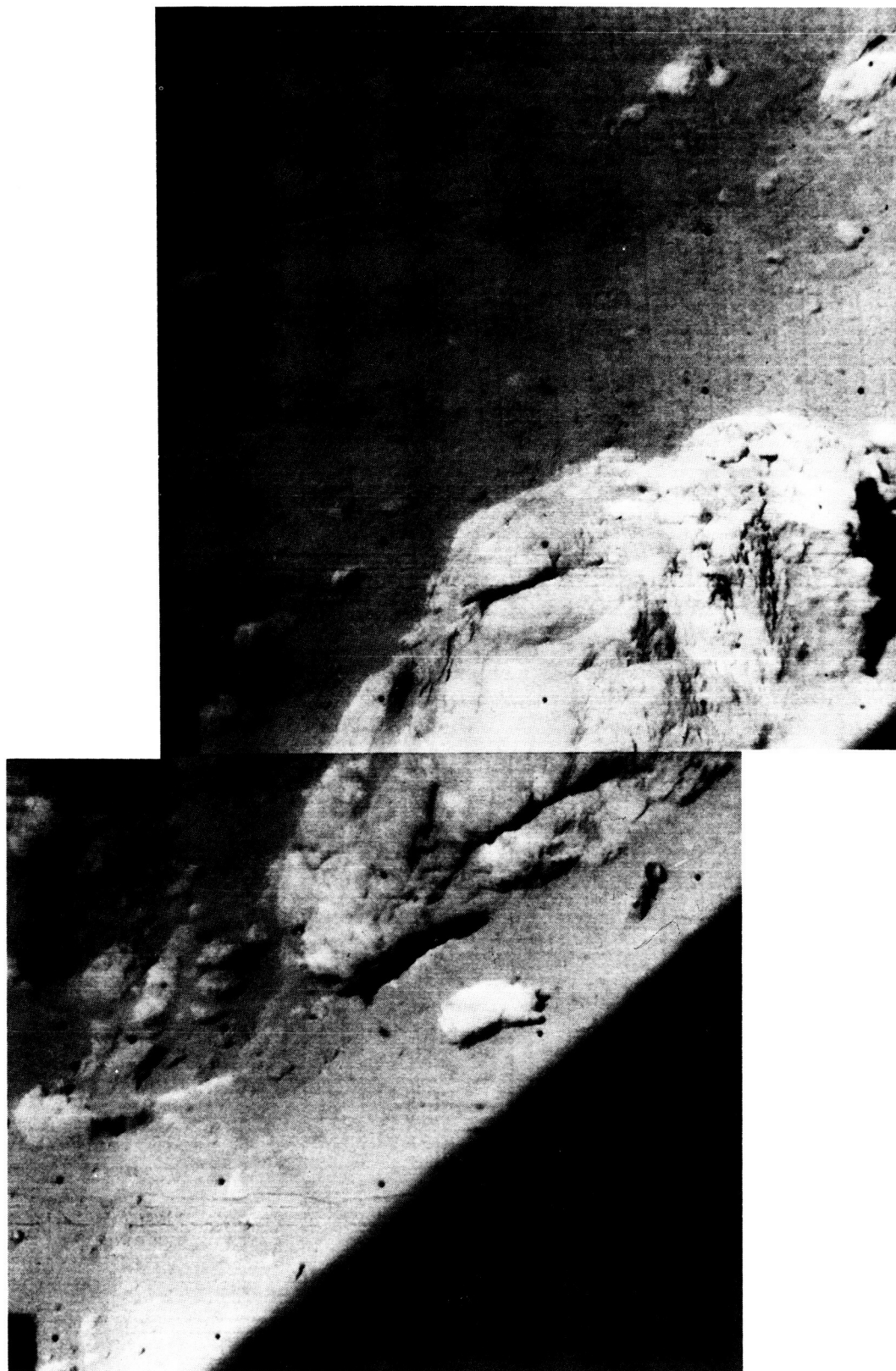


Fig. 3. Composite showing 6- x 18-in. rock approximately 12 ft from *Surveyor I*

total flight time was approximately 63 hr, 36 min, 37 sec. Confirmation of the soft landing was provided by: (1) the retention of DSS receiver lock onto the spacecraft transmitter signal, and (2) the low magnitude of the force telemetered by the shock absorber strain gages (<1600 lb, indicating touchdown velocities on the order

of 10 ft/sec). Telemetry was received continuously during touchdown.

At some time during the landing phase, probably at either retrorocket ignition or touchdown, the omnidirectional antenna A boom extended and the lock indication

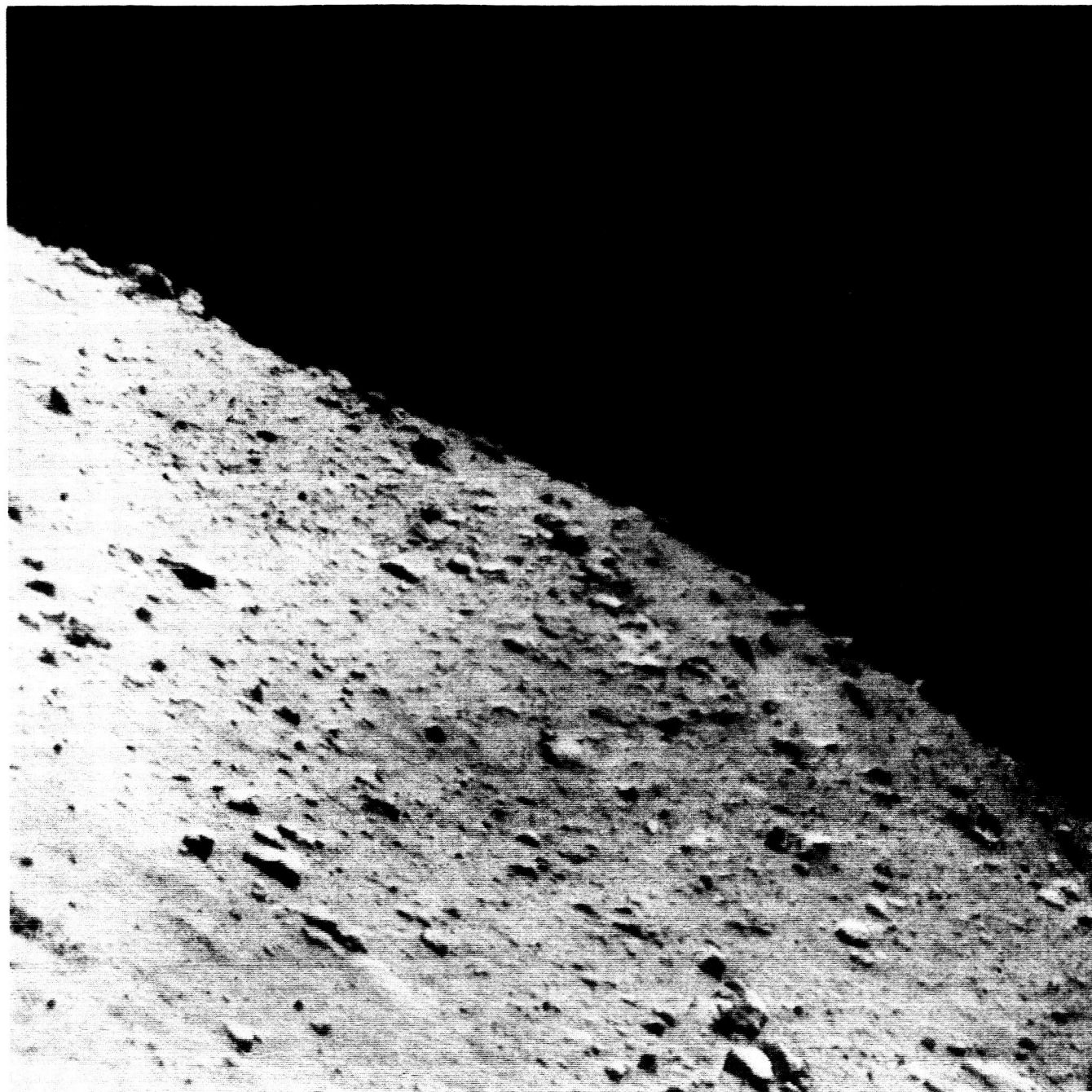


Fig. 4. Picture showing boulder-strewn lunar surface looking slightly south of east (camera-to-horizon distance estimated as several hundred yards)

came on. (The exact time cannot be determined since the lock indication telemetry is not on the commutator modes used during terminal descent.) The failure of omnidirectional antenna A to extend at the proper time at the spacecraft's separation from the *Centaur* stage presented essentially no problems during the mission, since all objectives were met using omnidirectional anteither retrorocket ignition or touchdown, the omnidirectional antenna B. Although center-of-gravity effects resulting from the improper position of omnidirectional antenna A were noted, these were small enough to be acceptable.

f. Postlanding. The TV camera was placed in operation a few minutes after the landing. The spacecraft performed as designed through the 12 Earth days remaining after landing until lunar sunset. On June 12, a loss of TV mirror deviation position telemetry occurred at one elevation position. On subsequent stepping, the mirror did respond and telemetry was obtained, thus indicating that the cause of the anomaly was simply a bad location on the elevation position readout potentiometer. This anomaly in no way impeded the taking of TV pictures. By June 14, 10,338 excellent-quality pictures of the *Surveyor I* spacecraft and its immediate vicinity had been obtained. Four of these pictures are shown in Fig. 1 through 4.

C. Systems Testing

SC-2 (second flight spacecraft) flight-acceptance tests. All preparations for the solar-thermal-vacuum tests were completed April 22. The first attempt at Phase 1A was aborted due to a liquid nitrogen leak which caused a premature shutdown. The second attempt was made after repair of the leak on April 23 and was entirely successful in attaining the desired environment, including a low solar intensity. Phase 1A was run as a 66-hr real-time mission sequence under a simulated solar-thermal-vacuum environment (including a low solar intensity of 87% of one solar constant for marginal thermal testing) on spacecraft power. System performance was satisfactory but the following two anomalies were noted: (1) main battery failure following the first terminal descent, and (2) Compartment A and B high temperatures. Due to the battery failure, a shutdown sequence was initiated following postlanding, TV, and troubleshooting operations. A new battery was installed, and Compartment A units and structure were replaced as required. Four thermal switches changed in Compartment A were reset to close at a lower temperature.

Phase 1B was started May 9, but was aborted at approximately 8 hr into the mission due to high temperatures in Compartment A and the main battery. The environment for this phase included a high solar intensity (112% of one solar constant). Three Compartment A switches were reworked due to foreign material found in one and assembly errors discovered in the other two.

On May 12, another liquid nitrogen leak was discovered during the pumpdown for Phase 2B (conducted at 112% of one solar constant). This prevented the chamber from attaining the specified pressure, but the stabilized pressure was sufficient to perform the mission. The spacecraft performed very well, thermally and functionally, during this phase. The exceptional performance of the batteries enabled them to support a standard mission sequence and one additional terminal descent. Anomalies included the following: (1) a short in the flight-control sensor group, (2) a temperature on a vernier line above the maximum allowable value, (3) a buildup of coating on the inside of the Canopus sensor window, and (4) abnormal operation of the null error amplifier in an analog-to-digital converter. Shutdown was initiated on May 16.

The flight-control sensor group and central signal processor units were removed for repairs and retest. Also, a switch on Compartment A was replaced. After return of the central signal processor units, the spacecraft was placed in the chamber, minus the flight-control sensor group, for chamber checkout related to the low vacuum in Phase 2B. Chamber pressure problems were checked out, and the spacecraft was subjected to 112% intensity for a brief period to determine if Compartment A switches and the vernier line which had previously caused problems were now functioning properly.

Following these special tests, the flight-control sensor group was installed on the spacecraft. Preparations for Phase 3B were completed May 31, and pumpdown was initiated. The mission sequence was successfully completed.

The Phase 1C mission sequence began June 11 and proceeded smoothly until a boost regulator failure during terminal descent resulted in a loss of communications with the spacecraft and a subsequent abort. The RADVS system remained on during this period and overheated after the boost regulator and RADVS were repaired. Phase 1C was rerun. Special tests were included to verify the proper operation of the boost regulator and RADVS.

SC-3 (third flight spacecraft) flight-acceptance tests. The SC-3 entered the initial system checkout test phase

on April 18. All major electronic units were installed, except for the flight-control sensor group, antenna and solar panel positioner, and radar altimeter and doppler velocity sensor. The testing was completed during this reporting period, except for those tests for the mechanisms and vehicle telecommunications which were delayed due to the late delivery of the antenna and solar panel positioner. Telecommunications intergroup integration, TV, flight-control, and flight-control altitude marking radar telecommunications tests and a number of special tests were performed. Both transmitters indicated phase jitter greater than that allowed by specification during the telecommunications integration phase. This problem is under investigation. During the TV and telecommunications testing, a failure was noted in the survey TV camera mirror drive assembly, necessitating rework and retesting of this assembly.

T-2N-1 and T-2N-2 (descent dynamics test vehicles) tests. One touchdown mission was successfully performed by each of these vehicles at Holloman Air Force Base. Preliminary analyses of test data indicate all primary and secondary test objectives were accomplished. Prior to these soft-landings, both vehicles had completed an altitude recovery test with touchdown modifications incorporated to demonstrate system readiness for the touchdown missions. The T-2N-2 also completed system functional and environmental tests after touchdown modification.

A roll loop gain reduction incorporated in both T-2N-1 and T-2N-2 was tested during the descent tests (two altitude recoveries and two touchdowns). The roll control loop was very stable throughout each of these tests and exhibited no tendency to limit-cycle or rate-saturate.

Both vehicles will be cycled through a final and complete system functional test sequence as a post-touchdown verification of subsystem status. When final optical data have been analyzed and it can be shown that all test objectives have been satisfactorily met, the T-2N testing program will be terminated.

S-15 (landing dynamic stability test vehicle) drop tests. The two-dimensional phase of the S-15 drop-test program was recently completed. A mechanical and electrical calibration of the complete S-15 instrumentation system was performed. As a result, the system was upgraded to assure acquisition of all data channels and to establish greater confidence in the system's accuracy. Neoprene rubber sheet was bonded to the vehicle footpads to obtain a higher friction coefficient than that previously achieved. The four drops which were then

made showed a higher degree of stability than had been predicted theoretically using a friction coefficient of 0.84 on the footpads. However, comparable stability was achieved analytically by reducing the friction coefficient by 5%. To define a stability boundary by drop tests, a further increase in apparent friction on the footpads was effected by placing 2-in. aluminum cubes on the landing surface. Then, 11 drops were made on this surface, and the corresponding analytical predictions gave a friction coefficient of 1.0 on the footpads. Although analytical results were again conservative, a stability boundary was achieved by the drop tests. To establish the degree of correlation existing between the analytical predictions and the test results, a computer program was written which uses test measurement of shock absorber and rigid leg forces to calculate the friction coefficient acting on the footpads.

D. Space Flight Operations

Telemetry downlink subsystem performance. Using a command and data handling console, special performance tests of the *Surveyor* downlink telemetry subsystem were conducted to determine the reason for bit error-rate scatter observed during the operation of various consoles. With the test setup shown in Fig. 5, three types of tests were conducted:

Electromagnetic interference susceptibility tests. The objectives were: (1) to define the most susceptible point

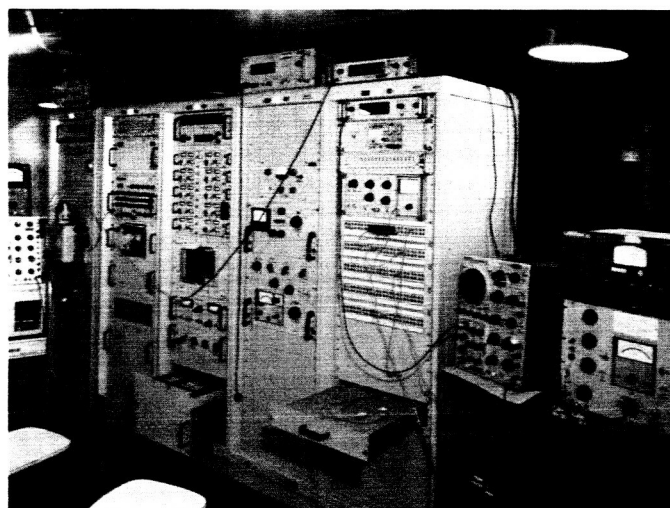


Fig. 5. Downlink telemetry subsystem test setup.

in the pulse-code-modulated telemetry link to conducted transient noise pulses, (2) to correlate susceptibility test data with bit-error-rate problems being experienced at command and data handling console field installations, and (3) to design and demonstrate simple engineering solutions for discrepancies uncovered during these tests.

The decommutator was found to be predominantly susceptible to negative transient pulses, which act like timing pulses causing transitions in the reconstructed pulse-code-modulated data which are randomly out-of-phase with the transitions of the input signal and associated normal timing pulses. These tests established that inadequate grounding exists in several locations and that significant improvement in bit-error-rate performance could be effected by using proper grounding techniques. After final ground modification, a complete series of bit-error-rate measurements as functions of bit rate and signal-to-noise ratio was made under conditions of bit-error-rate performance both with and without external pulses injected. At all bit rates, the increase in bit error rate was negligible when injecting pulses into the system.

Telemetry subsystem parameter optimization. The objectives were: (1) to characterize existing pulse-code-modulated downlink channel performance for all bit rates, for carefully controlled equipment setup conditions, and for a number of predetection signal-to-noise ratios; (2) to determine the variation of bit error rate with changes in nominal system parameter values or characteristics; (3) to determine the sensitivity of bit-error-rate measurements to equipment setups and procedures; and (4) to determine the sensitivity of bit error rate to nominal link element characteristic spread, i.e., bit error rate for several samples of channel selectors chosen from incoming acceptance lots so as to display, for instance, the maximum allowable divergence of bandwidth. The bit error rate was found to be essentially independent of postdetection filter characteristic and bandwidth, except for certain word patterns and the half-bit-rate bandwidth constant-amplitude filter situation. A noticeable dependence of bit error rate on word pattern may be due to the heavy premodulation filtering used in the existing pulse-code-modulated links. An extreme sensitivity of the 17.2-bit/sec channel to offset indicates that the link may prove unusable operationally due to setup and signal attenuation. A solution may be to use a wider bandwidth channel selector, sacrificing signal-to-noise ratio over portions of the mission sequence where possible to reduce the causes of this sensitivity.

Decommutator assessment. The objective was to determine the effect on bit error rate of the following

command and data handling console telemetry subsystem adjustments: pulse-code-modulated discriminator balance, decommutator input attenuator setting, and decommutator internal settings. As a result of the tests, it was recommended that the following be incorporated: (1) an adjustable bias circuit in the pulse-code-modulated amplifier, and (2) a new procedure at the stations for setting up the decommutator for processing pulse-code-modulated telemetry signals during a mission.

E. Electronics

Upper hemispherical antenna. Two upper hemispherical antenna configurations are being considered: The first would be a separate control item, similar to the omnidirectional antenna, which would be boom-mounted on the spacecraft. Although a straightforward design, this configuration would result in a greater spacecraft weight. The antenna would weigh about 0.28 lb plus the weight of the coaxial cable. To this must be added the weight of the boom and mechanisms required for attachment to the spacecraft. The second configuration would require an addition to the planar array antenna which would be permanently attached to and tested with the planar array. This configuration has the disadvantage that both antennas would have to be replaced should either of them require replacement. Also, structural loads on the planar array antenna would increase about 10%, resulting in the expenditure of a planar array antenna in providing type-approval test assurance for this design. The question of retest of retrofitted planar array antennas will also have to be considered. This configuration would result in a net spacecraft weight increase of about 0.20 lb plus the weight of the coaxial cable.

Pattern and impedance measurements were completed on an electrical prototype of an upper hemispherical antenna. The prototype differs from the breadboard antenna in that the ground plane of the prototype does not have a radial choke. Electrical performance of the antenna is very nearly the same with or without the choke. By omitting the choke, however, the weight of the antenna was reduced by more than 50%.

Antenna switch unit. An antenna switch is presently being designed to switch the secondary receiver between the upper hemispherical antenna and the existing omnidirectional antenna. This switch will provide circuitry to transfer a latching coaxial RF switch from one antenna

to the other. The coaxial-switch and associated drive circuitry are identical to that in the transmitter. The unit will weigh approximately 1.5 lb. The type-approval antenna switch is expected to be ready for testing in July.

F. Electrical Power Source

Solar panel design. A preliminary design of the solar panels for SC-5, -6, and -7 (the fifth, sixth, and seventh *Surveyor* flight spacecraft) has been completed, and fabrication of the first prototype hardware is under way. The design differs from that for SC-1 through SC-4 (the first four flight spacecraft) in that it incorporates the flat solar cell mounting technique rather than the rigid shingle concept. The new design is more rugged both thermally and mechanically and should improve confidence in the capability of the panels to survive the increased environmental requirements for these spacecraft.

The submodule used is very similar to that successfully used for the *Mariner IV* spacecraft solar panels: seven 1- × 2-cm, P/N, 1-ohm/cm, silicon cells connected in series-parallel by kovar bus bars. (Kovar is an iron, nickel, and cobalt alloy with thermal expansion characteristics similar to those of the silicon solar cells; its use will greatly reduce the effects of thermal shock and thermal cycling on cell interconnections.) The P/N cells planned for use on this panel are residual cells from the *Mariner Mars 1964* and *Ranger* Projects; thus, a significant amount of empirical data is available concerning the electrical and mechanical characteristics of the cells. Data for modules made for the prototype panel indicate that the nominal postfabrication efficiency for these panels will be the same as that for the *Mariner Mars 1964* panels.

G. Propulsion

Simulated lunar thrust-chamber-assembly firings. It was proposed that the vernier engines of *Surveyor* spacecraft be ignited after touchdown on the lunar surface in an attempt to disturb the surface. Additional data on the mechanical properties of the surface could thus be provided. To ascertain whether the vernier engines would ignite at all under the prevailing operating conditions and, if they would ignite, what sort of operation they would provide, two sets of two tests each were conducted. The tests were performed in an environmental

chamber capable of preconditioning the test engine and propellants to desired temperature and pressure levels.

In the first set of tests conducted June 6, the *Surveyor I* spacecraft conditions prevailing that evening were simulated so that it could be determined if engine ignition would occur and what thrust would result under these conditions. The second set conducted June 9 simulated the more favorable environmental conditions that would prevail for the spacecraft later that week. Because the previous tests indicated that the engine could be presumed to operate, these tests were intended to demonstrate the effect a vernier engine firing may have on the lunar surface. (Should soil be disturbed to such an extent that it deposited on critical areas such as temperature-control surfaces or the TV camera mirror, spacecraft operation would be seriously impaired.) The test setup is shown in Fig. 6. The soil used was chosen to simulate the particle-size distribution evidenced in previously transmitted *Surveyor I* pictures and also the

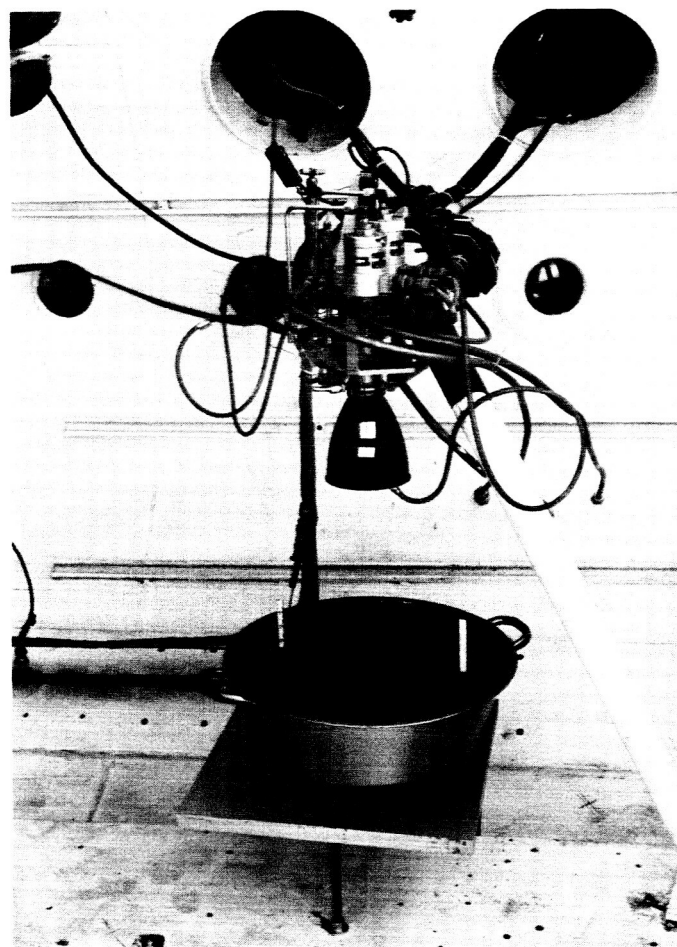


Fig. 6. Initial test setup for demonstrating the effect of a vernier engine firing on the lunar surface

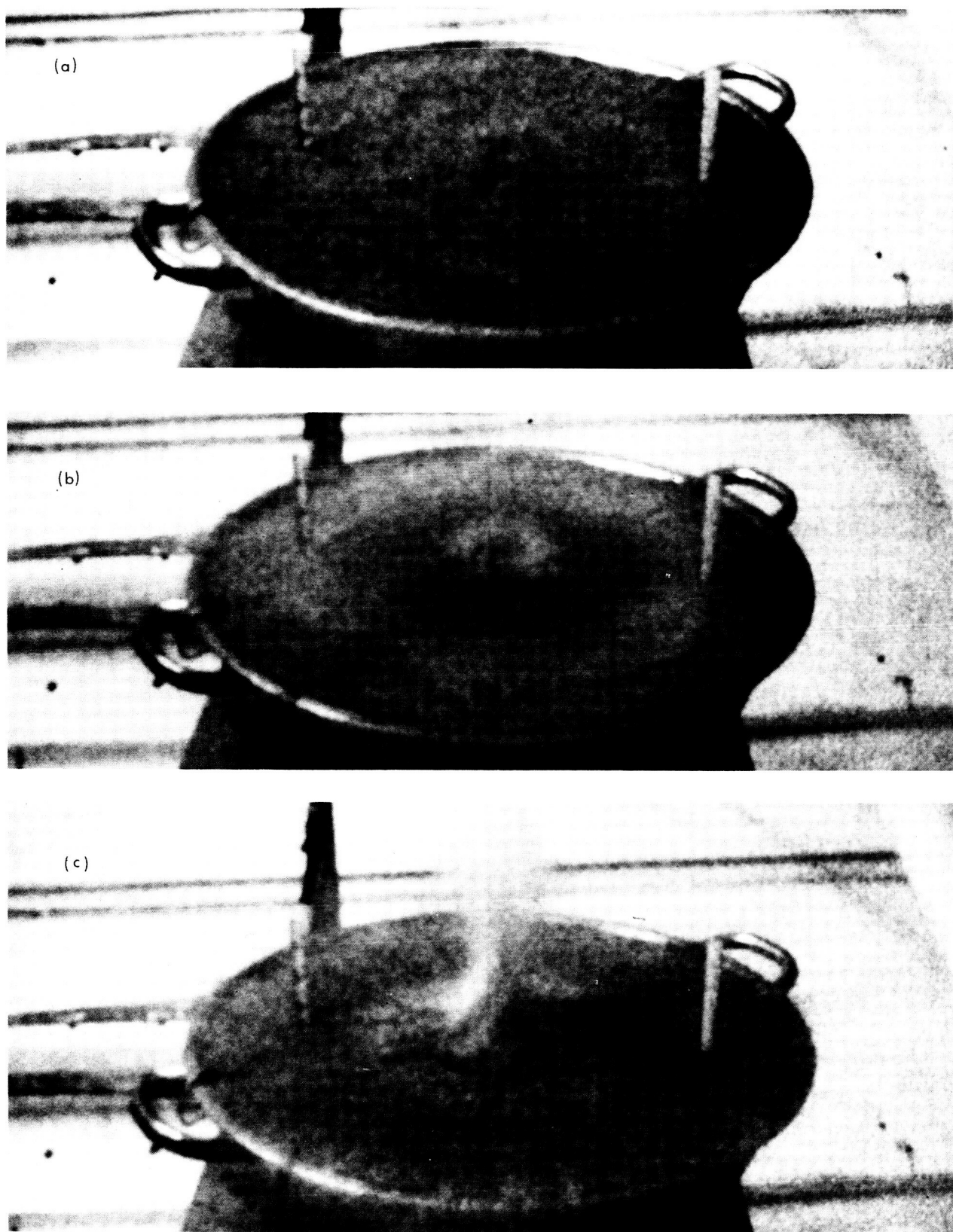


Fig. 7. Soil behavior during vernier engine firing

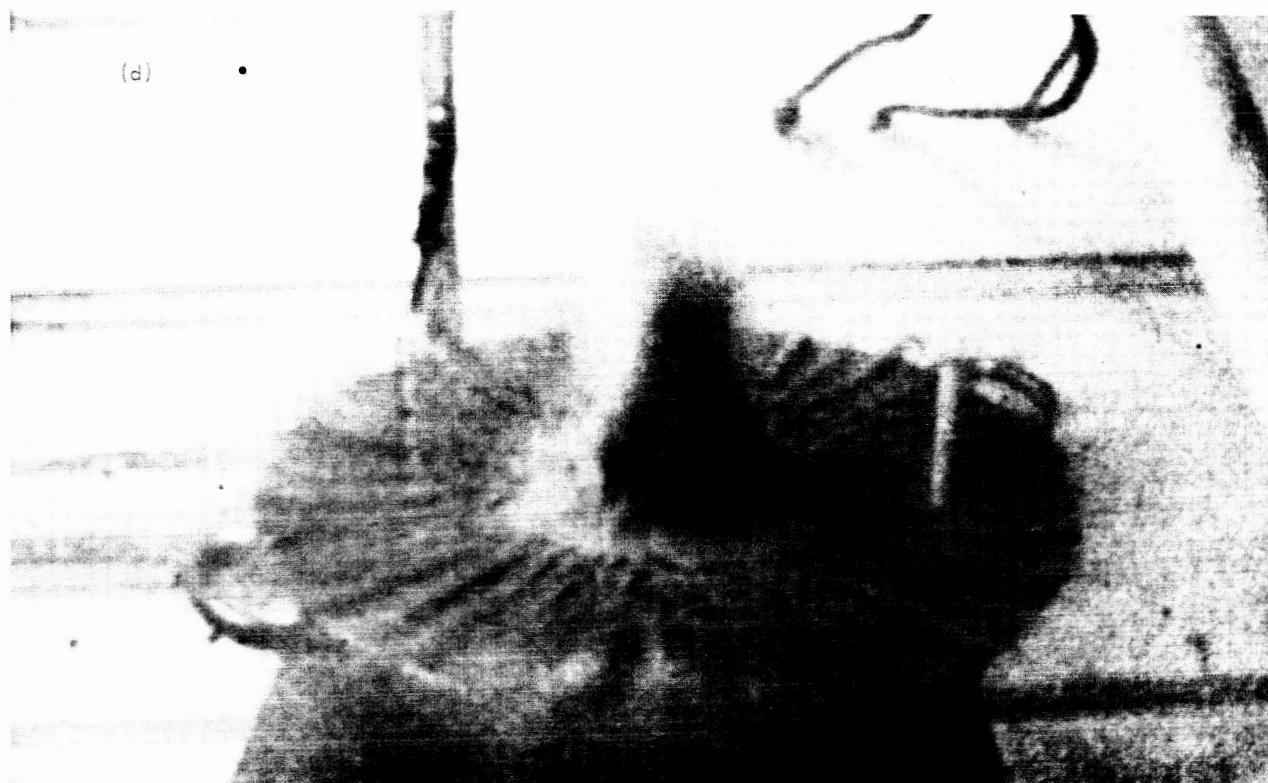


Fig. 7 (cont'd)

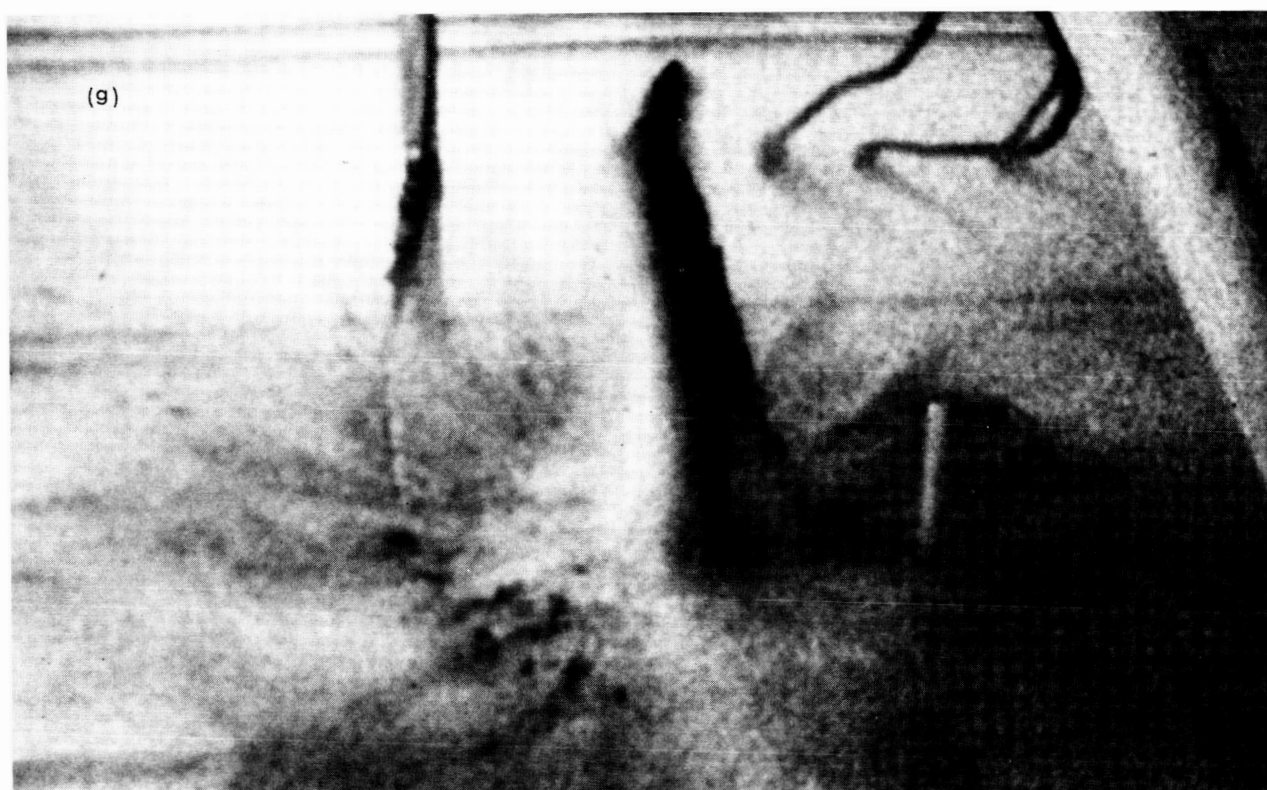
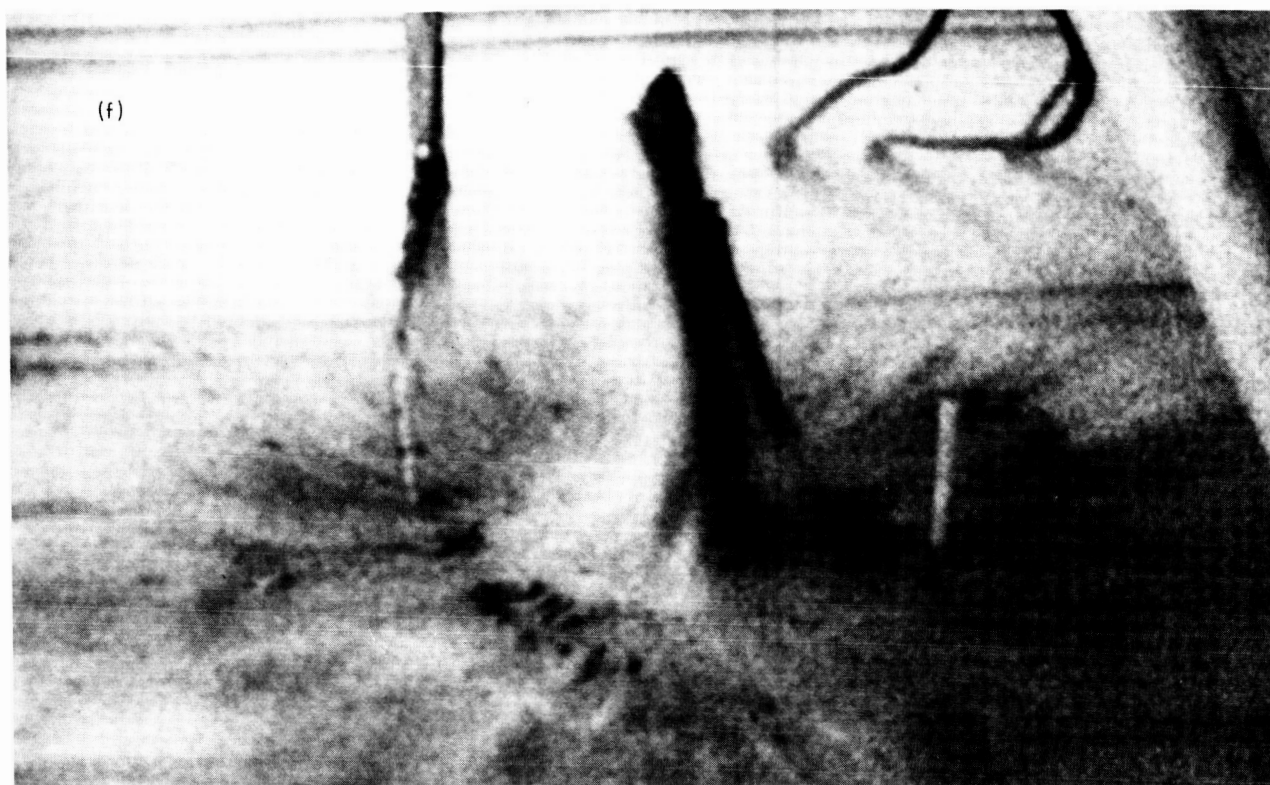


Fig. 7 (cont'd)

current "best guess" of the lunar surface bearing strength; however, the soil chosen was intentionally cohesionless to illustrate the effects of the engine thrust.

As a result of the engine firing, some soil was transported out of the chamber. The soil behavior is shown in Fig. 7, which gives frames of high-speed motion pictures taken during engine operation. The radial spray directed almost tangential to the surface conformed to the expected behavior, but the central column, which seemed to be stable, is unexplainable. This column at times rose to within 1 or 2 in. of the nozzle exit plane. A method-of-characteristics solution of the flow in the vernier engine nozzle is now being sought to determine if a local minimum in the soil pressure at the nozzle centerline could be caused by this engine's nozzle contour.

Although highly qualitative, the tests showed that the vernier thrust chamber assembly will operate at some of the off-design conditions existing on the lunar surface. There was sufficient energy in the exhaust to transport and raise to significant heights an appreciable quantity of the cohesionless soil tested. However, should lunar soil possess a significant amount of cohesion, there is little or no possibility that the force available would be sufficient to break the bonds. These tests indicate that an experiment of this nature performed on the lunar surface could be evaluated on Earth (less gravity effects) by simulating the lunar conditions at the time of firing in an environmental chamber, using models of the lunar surface as the variable parameter.

H. Payload and Scientific Mechanisms

TV camera mirror drive cable. Failure of the *Surveyor I* TV camera mirror drive to respond when commanded to move 118 azimuth steps prompted an investigation of the mirror drive cable to determine its thermal flexibility. Three various-size cable wires were evaluated by defining the net torque of each cable when the mirror drive was rotated in the specified manner and by observing how the amount of torque varied with changes in temperature, length and flexure of cable, and location of cable mount. The production cable, two redesigned cables, and the cable mount were tested to determine which would offer the least resistance to operation of the mirror assembly at room temperature and -100°F ambient.

Before undergoing solar-thermal-vacuum tests, SC-2 (second flight spacecraft) was modified to include one of the proposed cables and its corresponding method of attachment. The mirror drive cable or cable attachment configuration requires sufficient flexibility for rotational freedom in azimuth during solar-thermal-vacuum simulation as well as during the mission. Test results indicate that, by use of this proposed cable and its method of attachment, maximum torque to flex the mirror drive cable will be approximately 55% less, the average torque will be 50% less, and the minimum voltage to the stepper motor will be approximately 45% less. The proposed cable also results in 17.3% less twisting torque (referenced to the cable connector) than the production cable.

PLANETARY—INTERPLANETARY PROGRAM

II. *Mariner* 1967 Project

A. Introduction

The *Mariner* 1967 Project continues and extends the work of the previous *Mariner* Projects. Two elements of the Project are concerned with the *Mariner IV* spacecraft now in space, while a third is concerned with the Venus flyby mission in 1967.

Mariner Mars 1964 project. Residual activity of the *Mariner* Mars 1964 Project consists primarily of continuing analysis of tracking data, publication of results by the principal investigators, and preparation of final reports. However, periodic detection, recording, and commanding activities involving the *Mariner IV* spacecraft have been assigned to the Deep Space Network (DSN). Using elements of the experimental facilities at Goldstone Station and advanced R&D techniques, attempts are being made to communicate with the spacecraft. Results are published in SPS, Vol. III.

Mariner IV project. In the second half of 1967, *Mariner IV* will again be within the normal communication range of the DSN stations. At that time an attempt will be made to obtain additional telemetry data from *Mariner IV*. The *Mariner IV* Project comprises the preparation, support, and actual reacquisition of the spacecraft.

The objectives, authorized in December 1965, simultaneously with those for the Venus flight, have been established as follows:

The primary objective of the Mariner IV Project is to obtain scientific information on the interplanetary environment in a region of space further from the Sun than the orbit of Earth during a period of increasing solar activity in 1967, using the Mariner IV spacecraft still operating in orbit around the Sun.

The secondary objectives are to obtain additional engineering knowledge about the consequences of extended exposure of spacecraft equipment in the interplanetary space environment and to acquire experience in the operation of a planetary spacecraft after a prolonged lifetime in deep space.

Flight operations on this project (provided that a functioning spacecraft allows this to occur) will overlap the *Mariner* Venus 67 Project flight activities.

Mariner Venus 67 project. The major task of the *Mariner* 1967 Project is the Venus flyby mission, named the *Mariner* Venus 67 Project. The following mission objectives have been established:

The primary objective of the Mariner Venus 67 Project is to conduct a flyby mission to Venus in 1967 in order to obtain scientific information which will complement and extend the results obtained by Mariner II relevant to determining the origin and nature of Venus and its environment.

Secondary objectives are to acquire engineering experience in converting and operating a spacecraft designed for flight to Mars into one flown to Venus, and to obtain information on the interplanetary environment during a period of increasing solar activity.

With the authorizing of this project late in December of 1965, and the launch opportunity occurring in June 1967, the period available to the *Mariner Venus 67* Project for planning, design, test, and other flight preparation is 18 mo. Because of this minimum length of time, application, to the fullest extent possible, must be made of techniques developed from the experience of prior missions, and existing hardware must be utilized.

The single flight spacecraft, designated M67-2, is currently being prepared by converting the spare spacecraft (MC-4) that was built for the *Mariner Mars 1964* Project.¹

An *Atlas-Agena D* launch vehicle will inject the spacecraft into a 120-day transit trajectory. The launch readiness date has been set at June 10, 1967, with a 14-day launch period starting June 12. Ranging provisions have been authorized for this mission which will offer the possibility of considerably enhancing the celestial mechanics experiment. At encounter, an unusually sharp perturbation will occur.

Seven scientific experiments have been approved for the *Mariner Venus 67* mission:

The first experiment requires the use of only the RF transmission subsystem on the spacecraft, and the last one utilizes only the tracking doppler data derived from the RF carrier. Of the remaining five experiments, four are to be accomplished with the existing instrumentation, with only minor modifications. Only the dual-frequency radio propagation experiment of Stanford requires the incorporation of a new scientific instrument into the payload.

¹Portions of the proof test model (PTM) spacecraft and spares from the MM64 Project are also being prepared as a flight-support spacecraft (M67-1); there will be no PTM as such. The flight-support spacecraft will serve the double function of pseudo-PTM and backup spacecraft for qualifying spare subsystems.

Other changes to the basic spacecraft design are necessitated by the fact that the spacecraft will travel toward, rather than away from, the Sun and also because conversions must be made to accommodate revised encounter sequencing and science payload. In particular, modifications are needed in the following areas:

- (1) Scientific data automation system
- (2) Antenna pattern and orientation
- (3) Thermal control
- (4) Solar panel configuration
- (5) Planetary sensors

During the May-June reporting period, the design of the mission operations system (MOS, which controls the spacecraft through its defined mission activities) and its supporting facilities took form as the spacecraft system design effort entered a period of detail work. A series of design reviews helped establish the configurations of both the MOS and spacecraft systems. Subsystem tests of the former *Mariner Mars 1964* proof test model (PTM) were completed and the PTM was then disassembled and its components sent to cognizant JPL divisions.

As a result of increased concern about the degree of biological quarantine to be implemented on the mission, a parametric analysis is being made of the trade-offs between the probability of contaminating the planet (by impacting it with the launch vehicle or spacecraft) and other constraints on the trajectory (such as aiming point, attainment of scientific objectives, mission success, and other typical mission probabilities). Meanwhile, the *Agena* stage of the launch vehicle is being built to accommodate retro-rockets, should they be needed to achieve a satisfactory probability of maintaining planetary quarantine.

B. Systems

Systems-test-complex data system. An automatic data acquisition, processing and display system is being designed and procured for supporting *Mariner Venus 67* spacecraft system tests in the JPL Spacecraft Assembly Facility (SAF) and at the Eastern Test Range (ETR). The type of support will be essentially the same as that provided to the *Mariner Mars 1964* spacecraft system by the SAF computer data system (CDS).

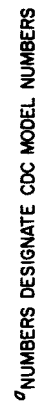


Fig. 1. Systems-test-complex data system

The CDS is not available for use by the *Mariner Venus 67* Project because it was transferred to the *Surveyor* Project shortly after the data system was returned to JPL following postlaunch support of *Mariner IV* at ETR. The CDS, together with additional similar systems based on the use of UNIVAC 1218 or 1219 computers, will continue to be used by *Surveyor* until conclusion of the project testing and launch support activities.

A new systems-test-complex data system (STCDS) is being developed for *Mariner Venus 67*, including subsystem elements for data acquisition and display (Fig. 1). The computer system (Control Data Corporation Model 3300) and all elements of the data display subsystem are leased equipment. Both the leased and the data acquisition equipment are being selected to provide continuing usefulness to other flight projects, particularly *Mariner Mars 1969*.

The computer system and portions of the data display subsystem are scheduled for delivery in late June 1966. Capability to process and display engineering and science telemetry data is planned for October 1966. The dates planned for providing further data acquisition and processing capabilities are: spacecraft and operational support equipment stimuli and responses, November 1966;

analog data from the spacecraft and from the STC facility and environmental sensors, January 1967.

<i>Experiment</i>	<i>Principal investigator</i>
S-Band radio occultation	Arvydas J. Kliore, Jet Propulsion Laboratory
Ultraviolet photometer	Charles A. Barth, University of Colorado
Dual-frequency radio propagation	Von R. Eshleman, Stanford University
Helium magnetometer	Edward J. Smith, Jet Propulsion Laboratory
Solar plasma	Herbert S. Bridge, Massachusetts Institute of Technology
Trapped radiation	James A. Van Allen, State University of Iowa
Celestial mechanics	John D. Anderson, Jet Propulsion Laboratory

III. *Mariner* Mars 1969 Project

A. Introduction

The *Mariner* Mars 1969 Project was initiated in late-December 1965 and formally tasked on February 1, 1966. The primary objective is to conduct two Mars flyby missions in 1969 to make exploratory investigations of the planet which will set the basis for future experiments — particularly those relevant to the search for extraterrestrial life. The secondary objective is to develop the technology needed for succeeding Mars missions.

The spacecraft design will be based on the configuration of the successful *Mariner IV* spacecraft, modified to meet the needs of the 1969 mission objectives and to enhance mission reliability.

The launch vehicle will be the *Atlas/Centaur* SLV-3C. This vehicle, developed under contract for and direction by the Lewis Research Center by General Dynamics/Convair, has a single- or double-burn capability in its second stage and a considerably increased performance rating over the *Atlas D/Agena D* used in the *Mariner IV* mission.

Mariner Mars 1969 missions will be supported by the Eastern Test Range launch facilities at Cape Kennedy, the tracking and data acquisition facilities of the Deep Space Network, and other NASA facilities.

The following planetary-science experiments have been tentatively (subject to integration capability) selected by NASA for the *Mariner* Mars 1969 missions:

- (1) Television: a two-vidicon, photometrically calibrated instrument. Partially overlapping, alternately green- and red-filtered, low-resolution pictures, and single-color, high-resolution pictures, each nested in a low-resolution overlap, will be taken. Both types of pictures will have an approximately 700- × 900-element format, with a factor-of-10 difference in resolution between them.
- (2) Infrared spectrometer: a two-channel, variable-filter-wedge transmission instrument with cooled, photon-activated, semiconductor detectors. Reflectance, emission, and absorption atmospheric and surface spectra from 1.5- to 15- μ wavelength with a spectral resolution of 100 will be acquired.

- (3) Ultraviolet airglow spectrometer: a two-channel, reflecting grating instrument with an occulting slit telescope and photomultiplier detectors. Resonance reradiation, fluorescence, absorption, particle-bombardment emission, and scattering atmospheric spectra from 1100 to 4500 Å with a 20-Å resolution will be acquired.
- (4) Infrared radiometer: a two-channel, dichroic-beam-splitter, interference-filter, infrared instrument with bimetallic thermopile detectors. Thermally emitted energy from the planet's surface will be radiometrically measured in two wavelength intervals: 8 to 12 μ and 18 to 25 μ .
- (5) S-band occultation: no flight instrument required. The doppler component of the S-band-telemetry communications signal during the occultation of the spacecraft by Mars will be analyzed to determine the spatial distribution of the index of refraction and the electron density of the planet's atmosphere.
- (6) Celestial mechanics: no flight instrument required. The trajectory tracking data during interplanetary transfer and at encounter will be analyzed to more accurately determine the value of the astronomical unit and the masses and ephemerides of Mars, the Earth, and the Moon.

The scientific investigators for the above experiments are listed in Table 1. The first four experiments will require instruments on the spacecraft that view Mars during the relatively brief period at encounter; data acquired at a high bit rate during this interval will be stored on magnetic tape for later transmission to Earth at a lower bit rate. The remaining two experiments require no flight instruments, but rely on trajectory data acquired by Tracking and Data Acquisition System equipment. No atmospheric-entry or cruise-science (for measurement of

Table 1. *Mariner Mars 1969* scientific investigators

Experiment	Scientific investigators	Affiliation
Television	R. B. Leighton*	California Institute of Technology (CIT)
	B. C. Murray R. P. Sharp N. H. Horowitz J. D. Allen	CIT CIT CIT Jet Propulsion Laboratory (JPL)
Infrared spectrometer	A. G. Herriman L. R. Malling R. K. Sloan N. Davies C. Leovy	JPL JPL JPL Rand Corporation Rand Corporation
	G. C. Pimentel*	University of California (UC), Berkeley UC, Berkeley
Ultraviolet airglow spectrometer	K. C. Herr C. A. Barth* W. G. Fastie	University of Colorado John Hopkins University
Infrared radiometer	G. Neugebauer* G. Munch S. C. Chase	CIT CIT Santa Barbara Research Center
S-band occultation	A. J. Kliore* D. L. Cain G. S. Levy	JPL JPL JPL
Celestial mechanics	J. D. Anderson*	JPL

*Principal investigator.

interplanetary phenomena) experiments will be carried on the *Mariner Mars 1969* spacecraft.

The following activities continued during this reporting period: general scientific payload studies, mission and spacecraft system design studies, and initial activities required for the eventual procurement of spacecraft subsystems from industry. (Design formulations are expected to begin during the next reporting period.) Specific studies related to particular scientific experiment requirements, instrument accommodation, and payload integration were initiated. In addition, preliminary studies of the interfaces with the launch vehicle and ground systems were conducted.

IV. *Voyager* Project

A. Introduction

1. Objectives

The primary objective of the *Voyager* Program is to carry out scientific investigations of the solar system by instrumented, unmanned spacecraft which will fly by, orbit, and/or land on the planets. Emphasis will be placed on acquisition of scientific information relevant to the origin and evolution of the solar system, the origin, evolution, and nature of life, and the application of this information to an understanding of terrestrial life. The primary objective of the *Voyager* mission to Mars, beginning in 1973, is to obtain information relative to the existence and nature of extraterrestrial life, the atmospheric, surface, and body characteristics of Mars, and the planetary environment by performing unmanned experiments on the surface of, and in orbit about, the planet. A secondary objective is to further our knowledge of the interplanetary medium between the planets Earth and Mars by obtaining scientific and engineering measurements while the spacecraft is in transit.

2. Project Plan

All *Voyager* missions will be conducted as events of an integrated program in which each individual flight forms a part of a logical sequence in an over-all technical plan of both lander and orbital operations. The *Voyager* design will provide for the carrying of large scientific payloads to the planet, telemetering of a high volume of data back to Earth, and long useful lifetimes in orbit about the planet and/or on the planetary surface. Hardware will be designed to accommodate a variety of spacecraft and/or capsule science payloads, mission profiles, and trajectories. Particular emphasis will be given to simple and conservative design, redundancy wherever appropriate, and a comprehensive program of component, subsystem, and system testing.

Over-all direction and evaluation of the *Voyager* Project is the responsibility of the Office of Space Science and Applications (OSSA) of the National Aeronautics and Space Administration (NASA). Management of the *Voyager* Project and implementation of selected systems is

the responsibility of the Jet Propulsion Laboratory (JPL) of the California Institute of Technology (CIT).

3. Technical Description

Two *Voyager* planetary vehicles are to be designed, constructed, and tested for launch on a single *Saturn V* during the 1973 Mars opportunity. Attention is also being given to requirements imposed on such vehicles by launches subsequent to 1973, such as a similar mission planned for 1975. Each planetary vehicle is to consist of a flight spacecraft and a flight capsule with science experiments conducted in 1973 both from the orbiter and on the planetary surface. The flight spacecraft with its several hundred pounds of science payload will weigh approximately 2500 lb; its retropropulsion subsystem may additionally weigh up to 15,000 lb. and the flight capsule will weigh about 3000 lb, or less. The flight spacecraft will be a fully attitude-stabilized device utilizing celestial references for the cruise phase, and will be capable of providing velocity increments for midcourse trajectory corrections and for Mars orbit attainment by both the flight spacecraft and flight capsule. Onboard sequencing and logic will be provided, as well as ground command capability. The flight spacecraft will supply its own power

from solar energy or from internal sources and will be capable of maintaining radio communications with Earth. In addition, the flight spacecraft will be thermally integrated and stabilized and will monitor various phenomena near Mars and during transit, and telemeter this information back to Earth; it will also monitor and telemeter data pertaining to spacecraft operation. The flight spacecraft will also provide the flight capsule with services such as power, timing and sequencing, telemetry, and command during the transit portion of the missions and may also serve as a communications relay. The sterilized flight capsule will be designed for separation from the flight spacecraft in orbit, for attaining a Mars impact trajectory, for entry into the Mars atmosphere, descent to the surface, and impact survival, and for surface lifetimes of two days in 1973 and later goals of as much as 6 mo. The flight capsule will contain the power, guidance, control, communications, and data handling systems necessary to complete its mission.

No deep space-flight tests of the flight spacecraft are planned, and compensation will be made by additional ground tests conducted to the extent possible. The test program for the flight capsule, which is planned to include Earth-entry flight tests, will investigate entry dynamics.

DEEP SPACE NETWORK

V. Introduction

The Deep Space Network (DSN), established by the NASA Office of Tracking and Data Acquisition, is under the system management and technical direction of JPL. The DSN is responsible for two-way communications with unmanned spacecraft travelling from approximately 10,000 miles from Earth to interplanetary distances. Tracking and data-handling equipment to support these missions is provided. Present facilities permit simultaneous control of a newly launched spacecraft and a second one already in flight. In preparation for the increased number of U.S. activities in space, a capability is being developed for simultaneous control of either two newly launched spacecraft plus two in flight, or four spacecraft in flight. Advanced communications techniques are being implemented to make possible obtaining data from, and tracking spacecraft to, planets as far out in space as Jupiter.

The DSN is distinct from other NASA networks such as the Scientific Satellite Tracking and Data Acquisition Network (STADAN), which tracks Earth-orbiting scientific and communication satellites, and the Manned Space

Flight Network (MSFN), which tracks the manned spacecraft of the *Gemini* and *Apollo* programs.

The DSN supports, or has supported, the following NASA space exploration projects: (1) *Ranger*, *Surveyor*, *Mariner*, and *Voyager* Projects of JPL; (2) *Lunar Orbiter* Project of the Langley Research Center; (3) *Pioneer* Project of the Ames Research Center, and (4) *Apollo* Project of the Manned Spacecraft Center (as backup to the Manned Space Flight Network). The main elements of the network are: the Deep Space Instrumentation Facility (DSIF), with space communications and tracking stations located around the world; the Ground Communications System (GCS), which provides communications between all elements of the DSN; and the JPL Space Flight Operations Facility (SFOF), the command and control center.

The DSIF tracking stations are situated such that three stations may be selected approximately 120 deg apart in longitude in order that a spacecraft in or near the ecliptic

plane is always within the field of view of at least one of the selected ground antennas. The DSIF stations are:

Deep Space Communication Complex (DSCC)	Deep Space Station (DSS)	DSS serial designation ¹
Goldstone	Pioneer	11
	Echo	12
	Venus	13
	Mars	14
Canberra ²	Woomera	41
	Tidbinbilla	42
	Booroomba ³	43
	Johannesburg	51
Madrid ²	Robledo	61
	Cebreros ⁴	62
	Rio Cofio ³	63
	Cape Kennedy (Spacecraft Monitoring)	71
	Ascension Island ⁴ (Spacecraft Guidance and Command)	72

¹As of June 1966, DSIF serial designations (e.g., DSIF-11) are no longer used.
²Planned.
³Station not yet authorized.
⁴Station not yet operational.

JPL operates the U.S. stations, and will operate the Ascension Island Station. The overseas stations are normally staffed and operated by government agencies of the respective countries, with the assistance of U.S. support personnel.

The Cape Kennedy Station supports spacecraft final checkout prior to launch, verifies compatibility between the DSN and the flight spacecraft, measures spacecraft frequencies during countdown, and provides telemetry reception from lift-off to local horizon. The other DSIF stations obtain angular position, velocity (doppler), and distance (range) data for the spacecraft, and provide command control to (up-link), and data reception from (down-link), the spacecraft. Large antennas, low noise phase-lock receiving systems, and high-power transmitters are utilized. The 85-ft diameter antennas have gains of 53 db at 2300 MHz, with a system temperature of 55°K, making possible the receipt of significant data rates at distances as far as the planet Mars. To improve the data rate and distance capability, a 210-ft diameter antenna has been built at the Goldstone Mars Station, and two additional antennas of this size are planned for installation at overseas stations.

In their present configuration, all stations with the exception of Johannesburg, are full S-band stations. The Johannesburg receiver has the capability for L- to S-band

conversion. The Ascension Island Station will be basically full S-band when it becomes operational.

It is the policy of the DSN to continuously conduct research and development of new components and systems and to engineer them into the network to maintain a state-of-the-art capability. Therefore, the Goldstone stations are also used for extensive investigation of space tracking and telecommunications techniques, establishment of DSIF/spacecraft compatibility, and development of new DSIF hardware and software. New DSIF-system equipment is installed and tested at the Goldstone facilities before being accepted for system-wide integration into the DSIF. After acceptance for general use, it is classed as Goldstone Duplicate Standard (GSDS) equipment, thus standardizing the design and operation of identical items throughout the system.

The GCS consists of voice, teletype, and high-speed data circuits provided by the NASA World-Wide Communications Network between each overseas station, the Cape Kennedy Station, and the SFOF. Voice, teletype, high-speed data, and video circuits between the SFOF and the Goldstone stations are provided by a DSN microwave link. The NASA Communications Network is a global network consisting of more than 100,000 route mi and 450,000 circuit mi, interconnecting 89 stations of which 34 are overseas in 18 foreign countries. It is entirely operationally oriented and comprises those circuits, terminals, and switching equipments interconnecting tracking and data acquisition stations with, for example, mission control, project control, and computing centers. Circuits used exclusively for administrative purposes are not included.

During the support of a spacecraft, the entire DSN operation is controlled by the SFOF. All spacecraft command, data processing, and data analysis can be accomplished within this facility. The SFOF, located in a three-story building at JPL, utilizes operations control consoles, status and operations displays, computers, and data-processing equipment for the analysis of spacecraft performance and space science experiments, and communications facilities to control space flight operations. This control is accomplished by generating trajectories and orbits, command and control data from tracking and telemetry data received from the DSIF in near-real time. The SFOF also reduces the telemetry, tracking, command, and station performance data recorded by the DSIF into engineering and scientific information for analysis and use by scientific experimenters and spacecraft engineers.

VI. Facilities and Development

High-Power Continuous Wave S-Band Traveling Wave Resonator (TWR). The microwave test facility (MTF) personnel at Goldstone have been engaged in the design and development of a TWR capable of obtaining up to 500 kw at 2113 MHz.

RF power is generated at 2113 MHz by a 5KM70SI klystron, which is part of the high-power test laboratory located at the MTF. After passing through the usual protective and monitoring circuitry, the signal is applied to the input tuner of the TWR through a high-power isolator.

The TWR is useful as a device to test low-loss high-power microwave components. Powers in excess of 450 kw at 2113 MHz can be obtained. The use of this resonator will allow the testing of microwave components such as switches, directional couplers, and filters at very high CW power level.

New Scientific Data Systems (SDS) Digital Computer Programs. The following four computer programs have been written by the systems data analysis group for scientific data systems (SDS) digital computers. They are presented as abstracts identified by their DSIF program library numbers.

External Display Test Program, DSIF Library No. DOI-5034-TP. The purpose of this program is to test two external display panels associated with the digital instrumentation subsystem. These panels are located in the station manager's console and in the receiver subsystem console.

In order to test all bit configurations possible, a set of ten numbers is generated. These numbers are then displayed with the four possible color combinations at a reasonably slow rate such that the operator may observe the displays.

This program will operate in the SDS 910 or 920 and takes approximately 2 min 15 sec to run a complete test.

Symbolic Paper Tape Editor, DSIF Library No. DOI-5022-OP. This computer program is a modified version of the standard SDS symbolic paper tape editor. The original SDS version was not a complete self-loading relocatable program and was impossible to use under certain circumstances. Therefore, the program was rewritten using symbolic language and provided with a relocatable bootstrap loader.

This program provides the following capabilities: (1) reproduction of paper tapes; (2) listing of paper tapes;

(3) generation of paper tapes from the keyboard console;
(4) insertion and deletion of specific records on a paper tape. The various options are controlled through use of the breakpoint switches and input control messages.

Real Time Star Track, DSIF Library No. DOI-5000-OP.
The real time star track program (RTST) computes data which can be used to compute coefficients for antenna

systematic pointing error functions that describe local hour angle and declination pointing errors.

Reformatting TTY Predicts to Magnetic Tape, DSIF Library No. DOI-5004-OP. The purpose of this program is to read tracking data predict tapes (TTY), check for transmission errors — correcting or deleting data accordingly, and reformatting the information for output to magnetic tape/or paper tape.

VII. Operational Activities

A. Station Preparation

Mars Deep Space Station. Installation of the S-band system in the second-floor control room of the antenna pedestal is progressing. Currently installed are the antenna servo, digital instrumentation, analog instrumentation, frequency and timing, recording, and system monitor console subsystems. These subsystems were used with the JPL and R&D maser for backup tracking of the *Surveyor I* passes and postlanding. Also installed are the system junction module, the maser/parametric amplifier ground controls, and the microwave switching units. Full operational testing of these units will be performed with complete system testing. The transmitter installation is nearly completed and partial testing is in progress.

The master equatorial antenna pointing subsystem arrived at the Mars DSS just prior to the dedication ceremonies April 29, and was thoroughly checked before installation in the room atop the instrument tower.

Echo Deep Space Station. The intersite microwave link between Mars and Echo DSS is completed and in operation. Installation of the telephone microwave by the California Interstate Telephone Company is progressing and is scheduled for a fall completion.

The multiple mission support area (MMSA) equipment is being installed for full, simultaneous support of the *Lunar Orbiter* and *Pioneer* missions. This equipment will provide duplicate analog instrumentation and associated multichannel tape recording subsystems, and will allow two stations to track different spacecraft simultaneously, while permitting one station to record the received data from both.

The S-band system microwave control racks were relocated early in June in preparation for the installation of the MMSA equipment.

Two FR-1400 seven-channel magnetic tape recorders were received in May and are currently undergoing operational tests.

Pioneer Deep Space Station. The Cebreros DSS equipment has been shipped from the Pioneer DSS to Spain, where further assembly and testing will be accomplished. Most of the Cebreros DSS personnel had also left Goldstone by the end of June.

Remodeling of the generator building continues, with reinstallation of two 150-kw generators and switchboards in progress. The 300-kw diesel generator mounted outside the generator building was used as the "U" bus prime

power during the *Surveyor I* mission, with commercial power backup.

Venus Deep Space Station. During the last week in June, construction of G-60, the laboratory and office building, was begun.

B. Flight Project Support

Surveyor I landed on the Moon at 23:17:00 Pacific Daylight Time and was under continuous surveillance and control by the Pioneer DSS. During passes one, two, and three, the Echo DSS tracked the spacecraft as backup command transmission, while the Mars 210-ft antenna tracked as a backup receive function. Microwave circuits integrated the three stations into a single unit.

Pioneer DSS participated in the postlanding picture-taking and experiments. During the first seven postlanding passes, the Pioneer DSS commanded and received data on the following:

- (1) The first ten 200-line TV pictures
- (2) Approximately 4000 600-line pictures
- (3) The gas jet surface dust experiment
- (4) The TV pictures of the star Sirius
- (5) The lunar surface color picture experiment

A total of over 10,000 pictures was received at the Pioneer DSS before the end of the lunar day on June 16.

Pioneer VI Project. The *Pioneer VI* spacecraft, which was launched on December 16, 1965, continues to be tracked by the Echo DSS. During the second pass, a Type II orientation was performed to position the spacecraft antenna relative to the Earth. Additional Type II orientations were performed in June. Since the thirtieth pass, tracking has been on a three- to five-day week basis. Late in May, tracking was reduced to approximately 8 hr a day because of the increased noise factor and parity error rates prevalent during the near-horizon attitudes.

The Mars DSS has tracked the *Pioneer VI* spacecraft for system tests and pointing accuracy of the antenna.

Initially, all tracking was performed with the R&D receiver. The reported use of a Goldstone duplicate standard (GSDS) maser with the R&D receiver was in error. The maser used at that time — and currently in use — was a JPL development model, tuneable between 2295 to 2388 MHz. Late in June, the *Pioneer VI* spacecraft was tracked by the Mars DSS with the GSDS receiver; transmission and command support were provided by the Echo DSS.

Lunar Orbiter Project. Final preparations for the *Lunar Orbiter* July launch and tracking were in progress at the Echo DSS during the last week of June. Culminating months of integrated system testing concurrent with the *Pioneer VI* mission, all Echo DSS operations personnel participated in a series of comprehensive training exercises. Three major areas were covered: the 3.2 and 3.3 series, including DSS mission procedural exercises; the 4.4 series of DSS simulation exercises, followed by a series of practice long countdown procedures; and the 5.1 series of operational readiness tests.

Mariner IV Mission. The Mars 210-ft. antenna, currently using JPL R&D receiving equipment, and, in conjunction with the Venus DSS, has successfully continued the tracking of the *Mariner IV* spacecraft. Venus DSS provided the up-link command capability through use of its 100-kw transmitter, and the necessary signal integration for receiving, at below and near threshold levels, Mars-tracked *Mariner IV* data during the Sun occultation experiment and subsequent tracking.

Mars DSS personnel, using the station digital instrumentation subsystem, assisted with the operation of the antenna servo drive and tracking predictions. On Sunday, June 5, commands were transmitted to and received by the spacecraft, thus establishing two-way lock resulting in two-way doppler. Additionally, telemetry and spectrograms were received from *Mariner IV*, approximately 188 million miles distant, and were forwarded to JPL for analysis.

C. Experimental Activities

The only experiments conducted at the Venus DSS during the period of April 14–June 13, 1966 were those involving reception of the *Mariner IV* spacecraft in cooperation with the Mars DSS. Maintenance, modifications,

upgrading, and cleanup were performed, with the station operating on a regular day-shift basis.

The cooperative tracking of *Mariner IV* took place May 3, May 21, and June 5, 1966. On each occasion,

telemetry was recorded on magnetic tape at the Mars DSS, and spectrograms were taken at the Venus DSS. A specially adjusted telemetry decommutator unit at JPL was successful in recovering telemetry from each of the above tracks, working from the magnetic tape recordings.

SPACE SCIENCES

VIII. Lunar and Planetary Instruments

A. Surveyor Single-Axis Seismometer Development

Single-axis seismometer development has been in progress since 1965. The primary objectives have been to design, develop, and fabricate flight quality hardware that (1) would satisfy the experiment operational requirements after having been subjected to the prescribed *Surveyor* type approval level environmental tests, and (2) would meet the *Surveyor* spacecraft interface requirements.

The experiment and scope of the specific activities that have been accomplished or are in progress are summarized below.

a. Instrument description. The *Surveyor* seismograph is composed of a single axis, short period (1-sec nominal period) vertical seismometer sensor, with a calibration circuit and amplifier to provide a properly conditioned signal for transmission. The seismometer sensor consists of a spring-supported inertial mass, which is the magnet of a magnet-coil velocity transducer. The coil is stationary

and fixed with respect to the frame of the transducer. The seismometer is electromagnetically damped, near critical, through the input impedance of the amplifier. The analog signal produced provides standard short and intermediate period seismic data.

- (1) **Sensitivity.** The seismograph system has the capability of detecting $1 \text{ m}\mu$ (10^{-9}) vertical motion at 1 Hz.
- (2) **Response.** The system response covers the range from $\frac{1}{20}$ to 20 Hz. Within this range, the instrument response is nominally that of a 1-sec, critically damped pendulum.
- (3) **Calibration.** The system is provided with a means of self-calibration through the incorporation of a known force to displace the seismic mass. This force is produced by passing a current through the calibration coil.
- (4) **Gain level.** Provisions are made for three separate gain levels, differing by a factor of ten, and obtainable on command. Gain level changes and calibration force changes occur simultaneously.

- (5) *Caging.* A method for caging the seismic mass during transit is provided to prevent transducer damage. Uncaging occurs on command after the spacecraft has completed touchdown.
- (6) *Mounting.* The seismometer sensor is supported within thermal shells by preloaded fiber glass support rings. The thermal support structure is then hard mounted to the spacecraft.
- (7) *Leveling.* The instrument sensor is capable of operation with the vertical spacecraft axis aligned vertically or rotated as much as 15 deg from the vertical at any azimuth angle.
- (8) *Temperature.* The seismometer electronics are functionally operational over the temperature range of -25 to $+150^{\circ}\text{F}$. The sensor is operational over the temperature range of -150 to $+300^{\circ}\text{F}$. The seismometer sensor temperature is monitored with an accuracy of $\pm 10^{\circ}\text{F}$; and a 1-w internal heater, switched by ground command, can provide temperature control when the sensor temperature falls below operating limits.

b. Engineering activities summary.

Instrument design. A breadboard model of the instrument intended to be incorporated in the *Surveyor* program was built by the principal investigator, Dr. G. H. Sutton, at Lamont Geological Observatory (LGO). The feasibility of the design was verified through extensive testing at LGO.

JPL, while working closely with LGO, assumed responsibility for delivering the project-required hardware. A brief description of several of the ancillary pieces of hardware used in the seismograph system is given below.

As stated above, the seismic mass has to be caged during the transit phases of the spacecraft to prevent transducer damage. This was accomplished by attaching a retractable ball to the mass assembly, which is then pulled downward and forced against the lower housing of the sensor assembly with approximately 600 lb of force. Two pistons in the cable release assembly collar the ball and prevent it from retracting.

During uncaging, two squibs are fired which force the pistons away from the ball and, thus, allow it to retract while freeing the mass assembly. The system reliability is increased by using redundancy. Uncaging would be accomplished if only one squib fired.

The reasons for designing and using an insulation assembly were to:

- (1) Provide a structure which supports the seismometer in the vertical and then facilitates mounting to the spacecraft.
- (2) Use the structure (thermal shells) for passive thermal control of the sensor.

In carrying out the design, it was necessary to consider the structure's weight, ability to survive the type approval environment, and make certain that it readily allowed access to the sensor. These objectives and constraints resulted in an insulation assembly consisting of three components:

- (1) Fiber glass support ring.
- (2) Thermal shells (upper dome and lower shell).
- (3) Support structure.

The sensor assembly is supported and separated from the near-spherical thermal shells by the conical fiber glass rings. Although the rings provide low thermal conductivity between the sensor and the shells, they are very strong. The thermal shells are then attached to the cylindrical support structure, which mounts to the spacecraft. Fig. 1 is a sketch of the seismometer insulation assembly.

In conjunction with trying to passively control the temperature of the seismometer, a development contract was given to General Electric Company (GE) for the design and development of radiation shields which would fit between the sensor assembly and the thermal shells (i.e., fill the gap created by the support rings). The purpose of the shields was to reduce, as much as possible, the heat loss from the sensor due to radiation without significantly increasing the conduction heat loss.

GE fabricated the shields in three assemblies to facilitate access to the sensor as well as allow easy installation. Basically, the shields consist of an optimum layer of Hastings aluminized mylar, which is aluminized on both sides.

The P1 assembly is cylindrical and fits around the cylindrical portion of the sensor and thermal shells. The P2 assembly fits between the upper dome and the sensor's upper housing. The P3 shield fits around the cable release assembly in the lower shell.

Instrument fabrication. After competitive bidding, a fixed-price contract was awarded in early fiscal 1966 to Marshall Laboratory for the fabrication of two prototype

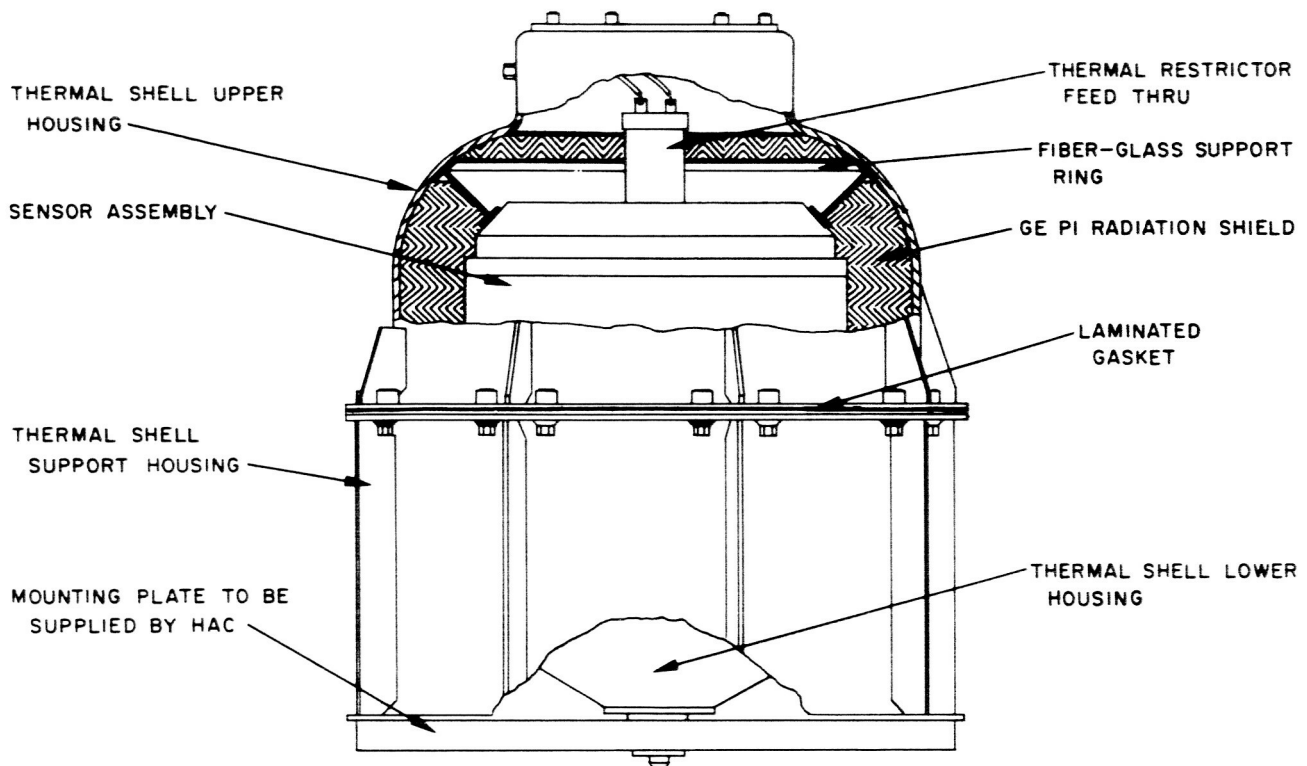


Fig. 1. Seismometer insulation assembly

and four flight instruments. The basic requirements of the contract were:

- (1) Fabricate all hardware to JPL-furnished drawings.
- (2) Use JPL preferred or Hi-Rel electronic parts.
- (3) Satisfy the quality assurance requirements outlined in JPL specification 30284.

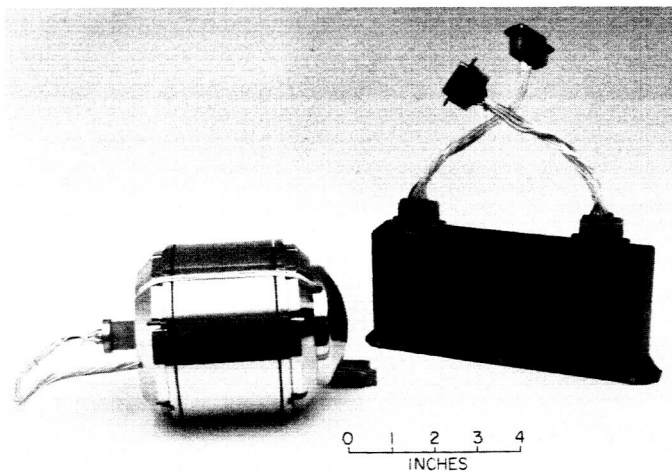


Fig. 2. Sensor and electronics assembly

The vendor received a "go-ahead" from JPL September 3, 1965, and on April 27, 1966, Marshall Laboratory delivered the last flight instrument to JPL.

Fig. 2 is a photograph of the sensor and electronics assembly. Fig. 3 is a photograph of the sensor during the assembly phase. The magnet mass assembly is shown being supported by the lower spring while the inductor coil legs are seen protruding from the mass assembly. The high quality of workmanship used in fabrication of the electronics is seen in Fig. 4.

The Missile and Space Division of GE was awarded a contract for the fabrication of six sets of flight quality radiation shields. GE had previously designed and developed a prototype set of radiation shields per the requirements discussed above. Prior to the follow-on contract, JPL performed extensive qualification tests on the prototype set.

Fig. 5 is a photograph of a typical flight quality PI radiation shield.

LaRae Industries, Hawthorne, California, which has extensive experience in machining and forming magnesium, was given a contract for fabrication of the insulation and

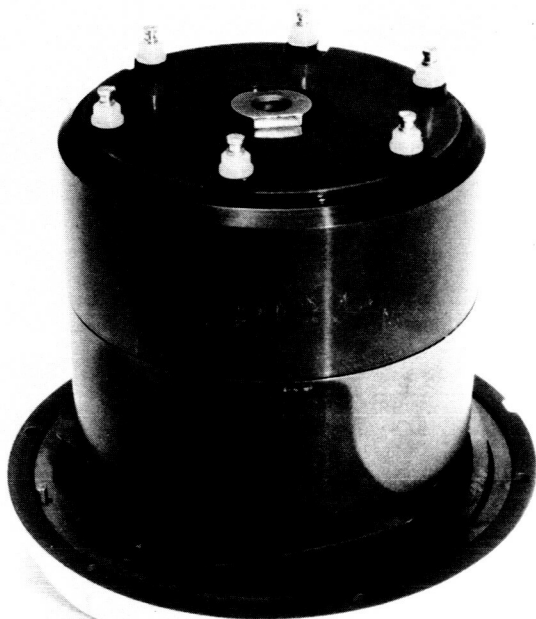


Fig. 3. Sensor mass and spring assembly

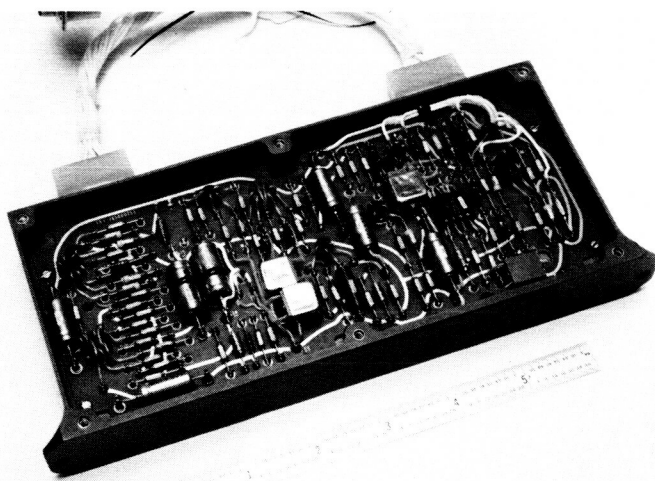


Fig. 4. Seismometer flight electronics circuit board and housing

support structure. All pieces of hardware were gold-plated, because gold provides a good substrate for possible future thermal coatings. A photograph of the upper dome is shown in Fig. 6.

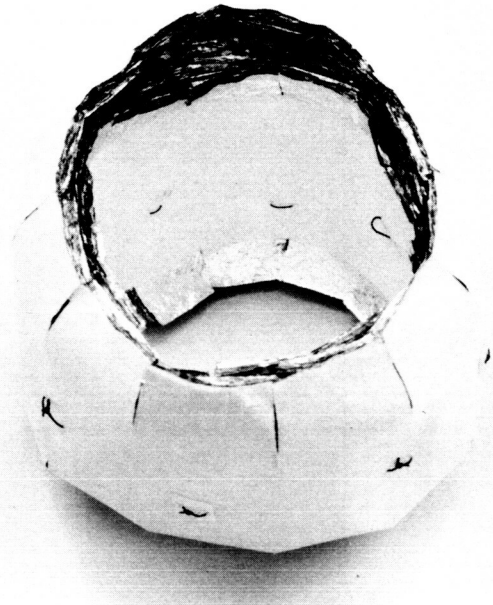


Fig. 5. Seismometer radiation shield P1 assembly

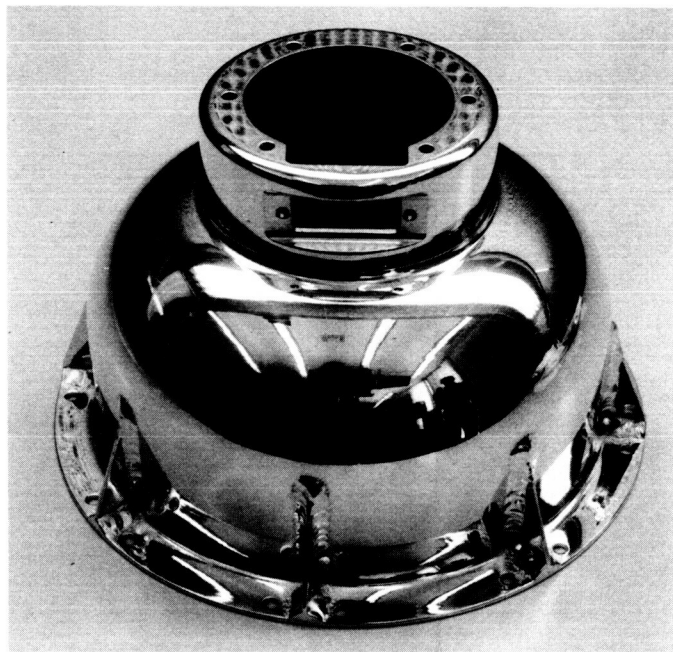


Fig. 6. Seismometer thermal shell upper dome

Responsibility for fabrication of the cable release assemblies remained with Division 38 of JPL. Fig. 7 is a photographed cross-section of a typical assembly.

The fiber glass support beams (Fig. 8) were made by World Plastics Corporation. They fabricated the beams

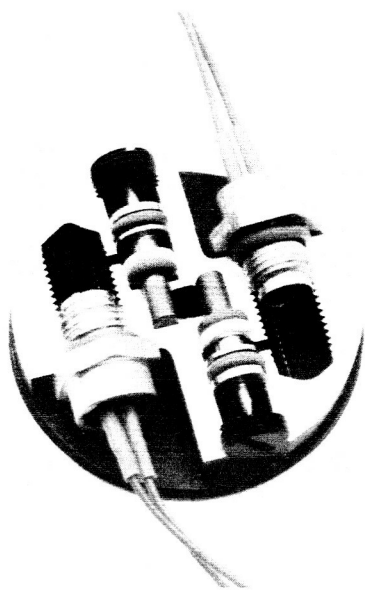


Fig. 7. Seismometer cable release assembly cut-away view

calibration/acceptance tests performed at Geotech Corporation. These tests were performed using a shaker table mounted on a seismic pier (Fig. 9). Instrument parameters such as (1) intrinsic voltage sensitivity; (2) damping; and (3) frequency response were recorded.¹ Fig. 10 contains typical frequency response curves of an instrument

¹All instruments were assembled with Earth-type springs which made testing the sensor in this manner possible.

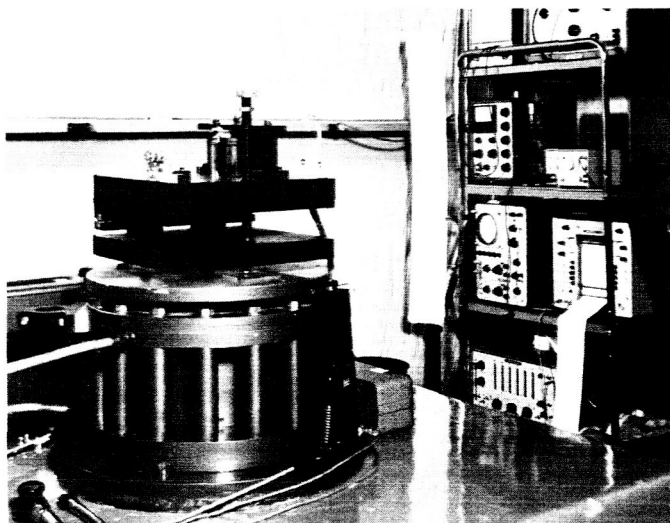


Fig. 9. Geotech calibration/acceptance testing

Fig. 8. Seismometer fiber glass support ring

in three pieces — top flange, continuous web, and bottom flange. The three pieces were then placed in a fixture and bonded together with Epon 828 resin.

Acceptance testing. Although final acceptance of sensor and electronic assemblies will depend upon future type approval test results, preliminary acceptance of the sensor assemblies from the vendor was based on the results of

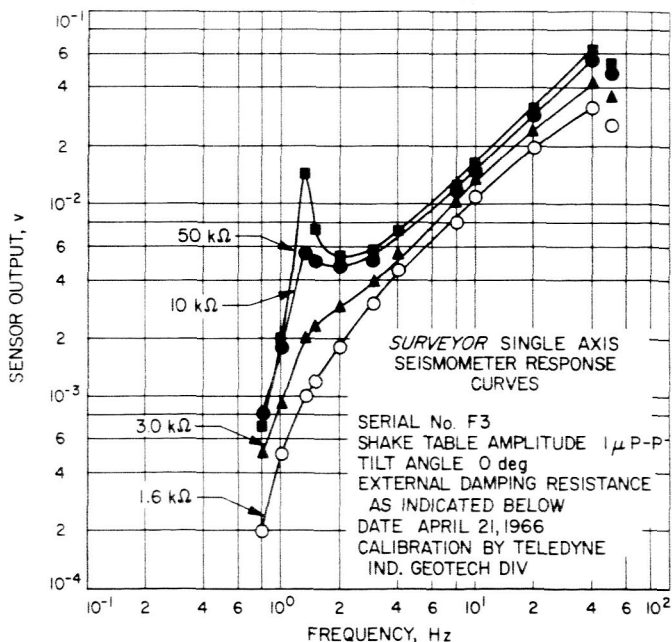


Fig. 10. Seismometer sensor frequency response curve

output coil which is shunted with varying damping resistors. The electronics acceptance tests were performed at Marshall Laboratory and included frequency response tests over the temperature range of -20 to $+150^{\circ}\text{F}$. JPL quality assurance and engineering personnel monitored and approved all tests.

Fig. 11 is a photograph of a flight *Surveyor* seismograph being tested with its associated bench checkout equipment, which has the capability of simulating all spacecraft commands.

Upon receiving the prototype radiation shields which had been designed and developed by GE, JPL installed them in the sensor thermal control model (TCM) insulation assembly and subjected the TCM to the following *Surveyor*-type approval level tests:

- (1) Thermal vacuum.
- (2) Three-axis vibration.
- (3) Thermal vacuum.
- (4) Thermal vacuum without radiation shields.

Fig. 12 contains temperature versus time graphs for the sensor's internal temperature recorded during each of the thermal vacuum tests. As the graphs indicate, the

radiation shields improve the thermal performance of the insulation and support package by approximately 100%. Degradation of the radiation performance after having been subjected to the vibration environment was

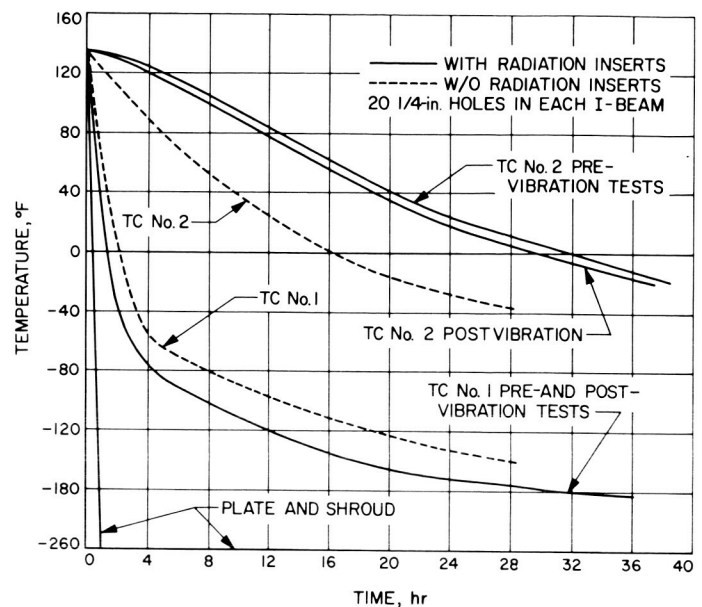


Fig. 12. Thermal vacuum test results—GE radiation shields

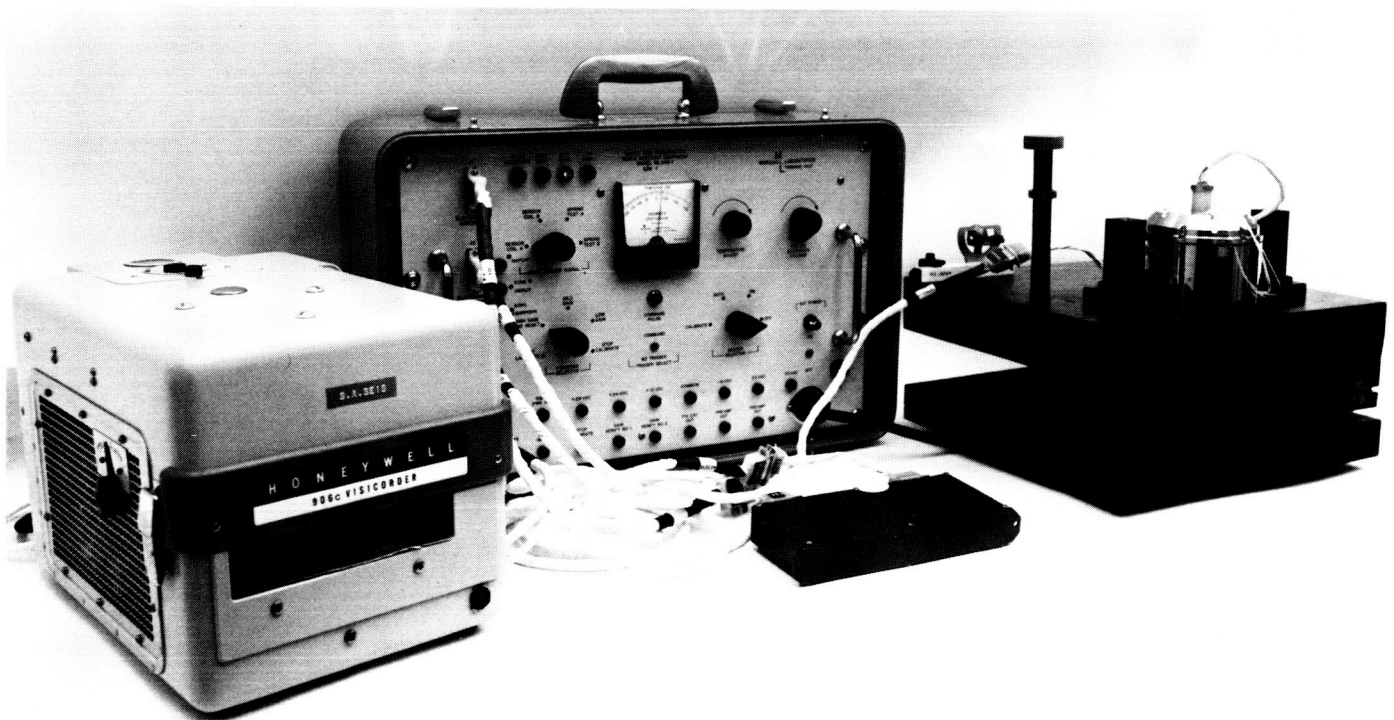


Fig. 11. Seismometer bench tests

less than 5%. The efficiency of the radiation shields approximated the value predicted by GE.

Elinvar Extra lunar spring development program. In parallel with the development of a satisfactory thermal control package for the sensor, a small research and development program has been carried on for the purpose of developing seismic lunar springs (i.e., springs whose mass support equals 5% that of Earth springs) whose parameters are insensitive to temperature.

Elinvar Extra (EE), a Hamilton Watch Company product, contains approximately 43% nickel with traces of cobalt, titanium and other metals. EE was selected as one of the more promising spring materials, since its thermal elastic coefficient of expansion is near zero, depending upon the heat treatments used. A contract was awarded to Hamilton Watch Co. in May 1965 to provide JPL with EE material, heat-treat facilities and technical support, as required.

After the springs are heat treated at Hamilton Watch Co., they are shipped to JPL and tested both singly and in pairs. Load versus deflection curves at ambient conditions are obtained for spring pairs from which decisions are made as to required changes in spring thicknesses, preform, or heat treatment.

The following combination of lunar springs has resulted in acceptable pairs:

- (1) 0.012-in. thick spring with preform -0.37 ± 0.020 in.
- (2) 0.014-in. thick spring with preform -0.62 ± 0.020 in.

Temperature tests on the EE and BeCu springs indicate that although BeCu lunar springs are usable with their characteristically large changes in natural period and mass support with temperature, calibration of the sensor is made much easier by using the EE springs, which have constant spring characteristics. EE lunar springs will be installed in all flight sensors.

IX. Space Instruments

A. *Mariner* Mars Magnetometer Configuration

The remaining *Mariner* Mars magnetometer flight units will undergo minor modification to update them to *Mariner* Venus 67 configuration. The scale is to be changed to ± 204.8 gamma from the previous ± 360 gamma.

A flux tank, which can be placed over the magnetometer sensor for nulling during systems and environmental testing, has been designed and placed on order. This will replace the coil system used previously and will provide for much quicker magnetometer checkout. Delivery is expected prior to the start of systems tests.

B. *Mariner* Venus 67 Trapped Radiation Detectors

The trapped radiation detectors were designed and fabricated at the State University of Iowa for the support of experiments by Prof. James A. Van Allen. The detectors were employed to search for magnetically trapped

particles in the vicinity of neighboring planets and to monitor the occurrence of solar cosmic rays and energetic particles in interplanetary space.

A version of the trapped radiation detectors was flown on *Mariner II*. This detector consisted of a collimated Geiger-Mueller tube detector with a mica end-window. It was capable of detecting electrons having the energy of $E_e > 70$ kev and protons with energy $E_p > 500$ kev. The axis of the detector located 70 deg from the spacecraft-Sun line, and the detector had a full field of view of 90 deg.

A second version of the trapped radiation detectors was flown on *Mariner IV*. This version consisted of three Geiger-Mueller tubes (Detectors A, B, and C) and a solid-state detector (Detector D). The axes of the collimated Detectors B, C, and D were parallel to each other at an angle of 70 deg to the spacecraft-Sun line. The axis of Detector A was located 135 deg from the spacecraft-Sun line. The solid-state detector was a surface barrier silicon device and, together with its electronics, provided two discriminated output levels, designated D1 and D2.

To prepare the trapped radiation detectors for flight in the present *Mariner* Venus 67 program, the MC-1 and MC-4 units built in the *Mariner* Mars 1964 program are

to be modified, calibrated, and tested. Requirements of the modifications and calibration were specified and a contract was awarded to the State University of Iowa for the following major modifications.

a. Instrument mounting. The spacecraft on a Venus trajectory will be such that the Sun is located on its $+z$ axis. In order for the various detectors to be properly oriented with respect to the Sun, the trapped radiation detector must be mounted on the spacecraft in an inverted configuration. A new mounting provision will be made so that the instrument can be attached to the spacecraft on the existing location on top of electronic Bay IV, with the instrument inverted 180 deg. The mechanical design of the new mounting brackets will be such that the existing mounting holes on the spacecraft can be used.

b. Detector A. The Geiger-Mueller tube, Detector A, pointing 135 deg from the spacecraft-Sun line will be relocated to point directly to the Sun. This will enable the instrument to measure soft X-rays below 14 Å, and

other charged particles emitted from the Sun. An extension bracket will be used to mount this detector. The mechanical design of the bracket will be such that no part of the spacecraft structure obscures the detector's 10-deg field of view.

c. Replacement of solid-state detector and incorporation of additional electronics. The existing solid-state silicon detector (Detector D) will be replaced by a new one having a wider range of response to the energy levels of the incident charged particles. The upper and lower energy portion channels will be extended to 20 and 0.25 Mev, respectively. The unidirectional geometric factor of the new detector will be increased approximately five times by using a detector of larger area. Additional electronics, including amplifiers and discriminators, will be incorporated at the detector output to provide four discriminated output levels designated as D1, D2, D3, and D4. By substitution of the new detector and electronics, a four-channel solid-state detector system (Fig. 1) is established in place of the existing two-channel system.

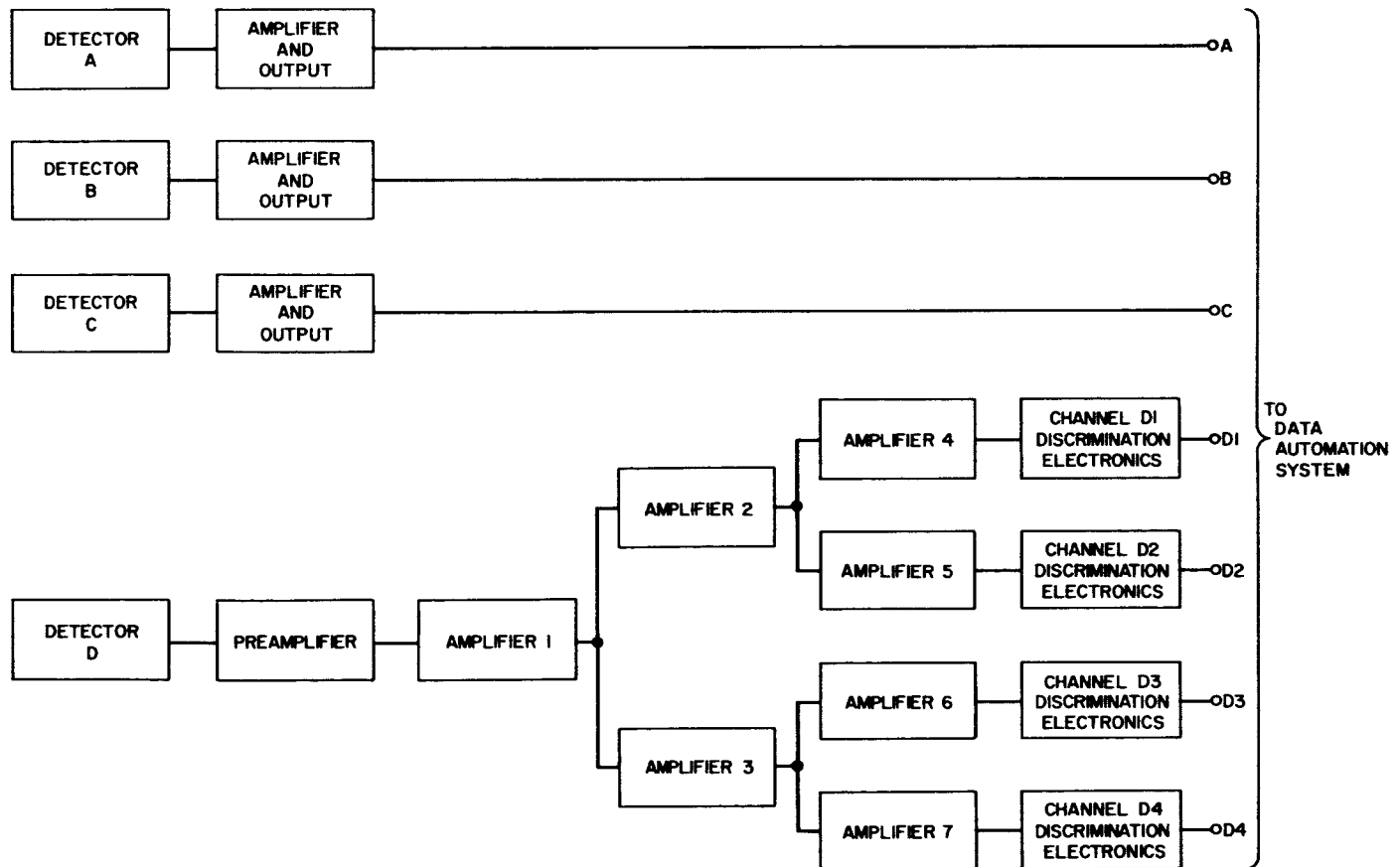


Fig. 1. Mariner Venus 67 trapped radiation detector functional block diagram

In addition to the three major modifications, a solar shield for the instrument will be required. The shield consists of layers of aluminized Mylar and aluminized Teflon and will be incorporated to shield the detector tubes from direct sunlight. A cutout will be made to provide a 10-deg field of view for the Sun-oriented Detector A. The solar shield, together with the proper thermal treatment of exposed surfaces, will be required to maintain the instrument operating within its temperature limits.

Flight acceptance tests, in accordance with the established JPL specification, will be performed on the modified flight instruments. A type approval instrument, incorporating all of the major mechanical changes, will be provided and will be subjected to the type approval vibration tests in accordance with established JPL specifications. Both type approval and flight acceptance testing will be performed at JPL.

C. A New Method for Recording Video Signals on Magnetic Tape

a. Photoscience camera techniques. A planetary photoscience camera must delineate surface features to the desired resolution and provide an accurate estimate of discrete illumination intensity. Of the three planetary photographic processes currently under consideration — chemical film, dielectric tape, and photostorage camera tubes — only the latter type performs directly as a photometer. With chemical film, the relationship between the luminous flux and the electrical read-out tends to become obscured, because light is transposed into the relatively inaccurate parameter density. During an actual mission, exposure of the film to the best Earth estimates proceeds until all frames are exposed. Only at some later time prior to transmission is the density information converted into an electrical signal. In the case of the photostorage camera tube, an electrical signal is generated from the photosurface directly after each exposure. This procedure not only is in the best interests of photometric accuracy, but also permits gain and exposure to be readjusted for optimum performance after each frame. The electro-optical transfer characteristics of the camera tube combined with encoded camera settings permit a direct transfer from luminous flux into electrical signal.

b. Data storage. The attention given to chemical film results primarily from its ability to read-in and store data instantaneously on the same film tape with both a wide-angle and a narrow-angle optical objective. The storage capacity of film is of the order of 6×10^6 bits/in.² Thus, a 500-line picture is instantaneously stored without loss of resolution on a 0.5-in. length of 16-mm film, where one ΔA picture element occupies 1 mil² and the information content $H = 1.5 \times 10^6$ bits. Planetary rate read-out presents problems, but it is not the subject of this discussion.

The preferred storage medium for the camera tube is magnetic tape. The photometric function is preserved to the accuracy of a quantized level when the video data are encoded on the tape in bit form. There is a negligible loss in accuracy when the tape is played back at the slowest planetary communication rates. However, problems arise with read-in rate and storage when the desired photographic information is increased, i.e., when the rate $R \gg 10$ kbits/sec and the frame information content $H \gg 10^5$ bits. A fast digital read-in rate may be accommodated by multiple-head recording. Thus, for the slow-scan 500-line image, 16 record heads can read-in data simultaneously on 16 tracks, on 1-in. tape at a 15-in./sec rate, to accommodate a data rate of 2.4×10^5 bits/sec. The storage capacity is then 1.6×10^4 bits/in.², requiring 100 in. of 1-in. tape per frame. However, in addition to its mechanical complexity, parallel recording requires reorganization of the serially produced video data, thus destroying the self-organizing feature of serial video data.

c. Analog recording. An alternative method of storing high-resolution signals is to revert to analog recording with a later transferral into the digital format prior to transmission. Conventionally, because of the DC component, analog video signals are recorded with a frequency-modulated (FM) system. However, FM introduces two new transfer functions: the FM modulator and the FM discriminator. Also, the FM carrier requires a high tape speed. To avoid these problems, a new approach has been developed which is based on a sampled data video signal. This approach was first described in SPS 37-38, Vol. VI, pp. 123–126.

Briefly, a sampled data video signal is produced by chopping the camera read-out beam at $2f_c$, where $f_c = \Delta t/2$ and Δt = the ΔA scanning time. The square-wave signal so produced is filtered, and the resultant is an AC modulated signal at frequency $2f_c$. The DC component is removed by capacitor coupling. When required for viewing or encoding, the DC component may be restored by inserting a DC restoring circuit. The varying-amplitude $2f_c$ signal is ideally suited for magnetic tape

recording. Recording at $2f_c$ permits a lower tape speed than the FM method since the FM carrier must be placed at $5f_c$. Elimination of the FM modulating and demodulating processes helps to preserve the accuracy of the photometric function.

The advantages of the sampling method over direct pulse-code-modulated recording for high-resolution pictures are that multiple-head stacks are avoided, and the data produced are on a simple in-line format. The read-in rate and the information packing density are both greatly

increased. The improved data compression results from two factors: First, digital encoding expands the data bandwidth. The expansion is directly related to quantization, so 6-bit encoding expands the bandwidth requirement by at least a factor of 6. Second, digital nonreturn-to-zero recording requires saturated tape signals for clear 0,1 identification. To ensure identification with multiple-track recording, the packing density is held to 1000 bits/lineal in. or 1 bit/mil. Sinusoidal data may be recorded at 3 cycles/mil, and a 10:1 packing gain is easily realized with a storage capacity of the order of 2×10^5 bits/in.².

d. Test results. To test the effectiveness of this new recording method, 500-line slow-scan pictures, generated by a vidicon camera, were processed to produce sampled

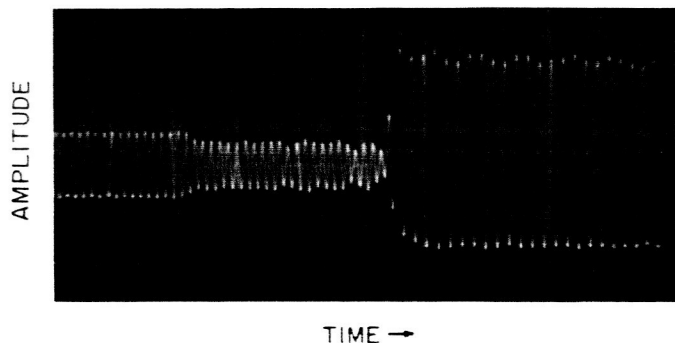


Fig. 2. 25-kHz sampled video signal (expanded view of small portion of line)

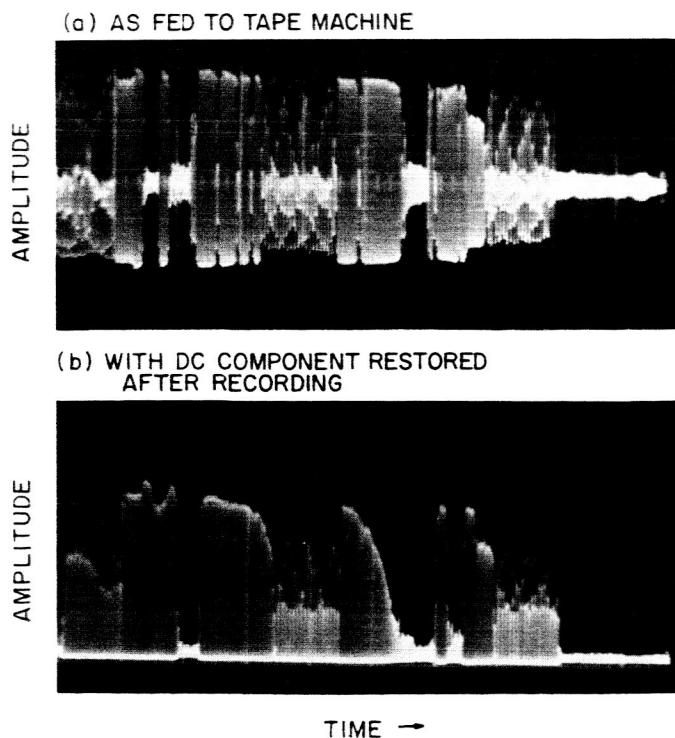
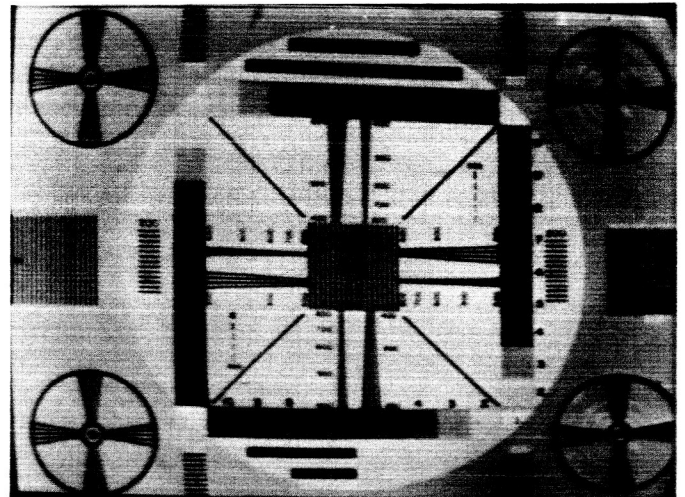


Fig. 3. One complete line of the 25-kHz sampled video signal

(a) DIRECT FROM VIDICON



(b) AFTER RECORDING

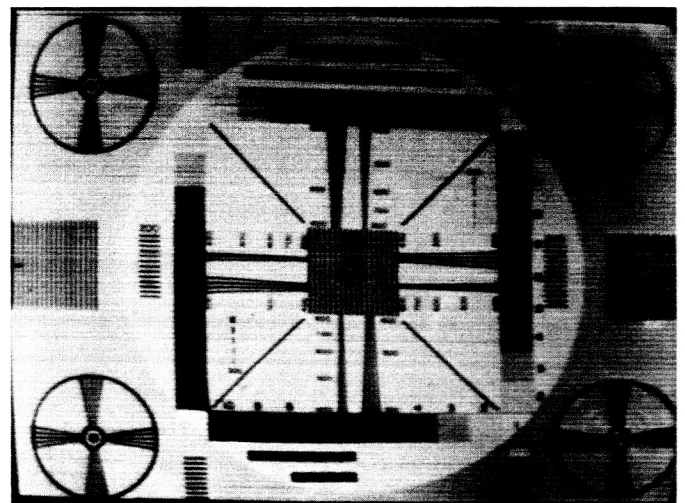


Fig. 4. Test pattern signals

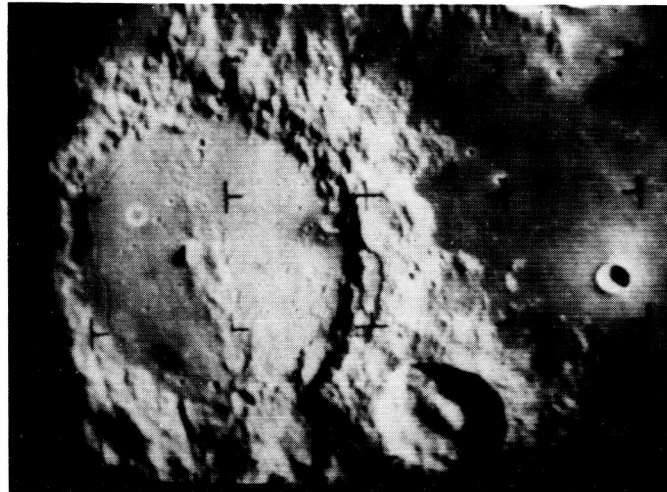
data signals which were fed into an Ampex CP-100 tape machine. With a frame time $T_f = 10$ sec and a line time $T_l = 20$ msec, $f_c = 12.5$ kHz and the vidicon beam-chopping frequency $2f_c = 25$ kHz. The frequency of the recorded tone was thus 25 kHz. On the Ampex CP-100, a tape speed of 15 in./sec can easily accommodate the 25-kHz tone. The measured electronic noise introduced by the recording process was negligible. The manufacturer's data indicated that the expected noise level at 25 kHz would be 50 db below the signal level. No attempt was made to optimize the equalization of the recording system over the narrow band of interest which should further enhance signals. Measurement indicated a flat response within 1 db over the operating range.

Polaroid photographs illustrate the performance. The 25-kHz amplitude-modulated sine-wave signal produced at the camera output is shown in Fig. 2 after filtering. This is an expanded view of a small section of a line covering about 60 ΔA elements. A complete line of the 25-kHz signal as fed to the tape machine is shown in Fig 3(a). The DC component is restored after recording in Fig. 3(b). The resolution before and after recording may be compared with the test pattern signals shown in Fig. 4(a and b). Resolution is scarcely affected, but a small variation in tape speed may be discerned. A similar comparison may be made with the view of Alphonsus given in Fig. 5(a and b), where no signal deterioration or tape-speed variation can be detected.

e. Conclusions. A new technique for processing camera signals has been described that permits direct analog recording of video signals on magnetic tape. The loss of resolution is negligible, particularly if the data must, in any case, be later digitally encoded. Both the read-in rate and storage capacity exceed those of direct digital recording by a factor of 10 or more. An advantage is in-line data recording at high read-in rates. Only the basic tech-

nique has been described here, but many variations and refinements of the method are possible.

(a) DIRECT FROM VIDICON



(b) AFTER RECORDING

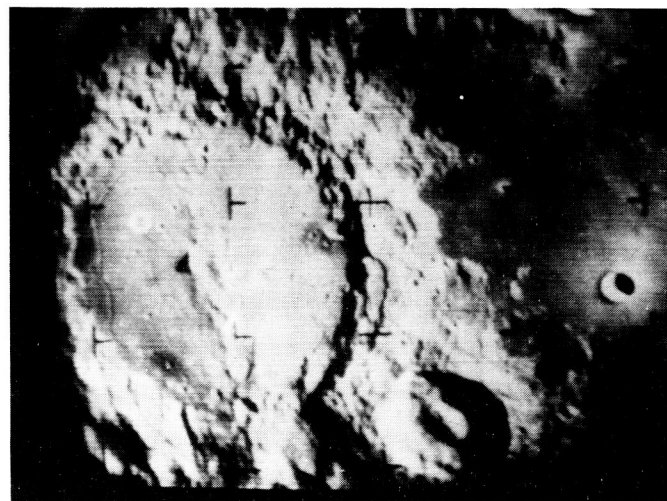


Fig. 5. Views of Alphonsus

X. Space Instrument Systems

A. Mariner Venus 67 Data Automation System

As an element of the science subsystem, the data automation system (DAS) sequences and controls the scientific instruments, receives, processes, and formats the scientific data, and sends it to other spacecraft subsystems for storage and transmission. The design of the DAS is determined by the instruments of the scientific payload, the operations they must perform, the data they produce, and in general the sequence of events which must occur in the science subsystem during flight, but especially during flyby of the planet. The data format and encounter sequence (illustrated in Sections B and XII(A), which follow) generally characterize the functional requirements to be met by the DAS. It is evident that the payload and the requirements change from project to project and necessitate practically complete logic and interface re-design of each DAS.

The major tasks in DAS design and development are determination of the interfaces, logic design to achieve the desired sequences and format, interface circuit design, logic proportionment in the mechanical design to accommodate the required functions within the packaging constraints, the actual mechanical and electrical de-

sign itself, and the subsequent fabrication and testing. Mission independence in DAS development is confined primarily to logic and circuit design approach, packaging approach, over-all format and timing approach, and fabrication techniques.

Four basic approaches to the DAS design were considered in the light of several stringent constraints. In addition to attaining high reliability, the development must proceed with a short schedule and an extremely tight cost constraint. The approaches used on *Mariners II* and *IV* were discarded early. The former would not meet weight and volume constraints; the latter utilized discrete pellet components and the precise types used on *Mariner IV* were not available on the allowable schedule, if at all. Two other approaches were available, however, and carefully examined. One of these uses discrete components in welded cordwood modules. Under a supporting research program, these modules have been developed with a view to producing a basic logic family of worst-case designed circuits and packages to provide a highly reliable and flexible unit. (SPS 37-32, Vol. VI, p. 49, and SPS 37-38, Vol. IV, pp. 127-135). Although this activity was well-advanced, even to the point of producing extensive process control documentation to ensure high-quality fabrication, weight and volume constraints resulted in selection of the fourth approach.

The approach adopted utilizes integrated circuits. Experience in flight projects had shown that these units could be used successfully in DAS-type functions. (SPS 37-31, Vol. IV, p. 215). A number of data processing and control circuits had been developed for the High Altitude Rocket Radar Project; these units had been developed to *Mariner C* environmental test requirements and they

performed perfectly. Additional experience with integrated circuits was gained in the development of the programmer portions of the OGO-E Plasma Probe and in the scan system of *Mariner C*. An additional advantage of this approach is that material costs for controlled or screened parts are significantly less for integrated circuits than for discrete components.

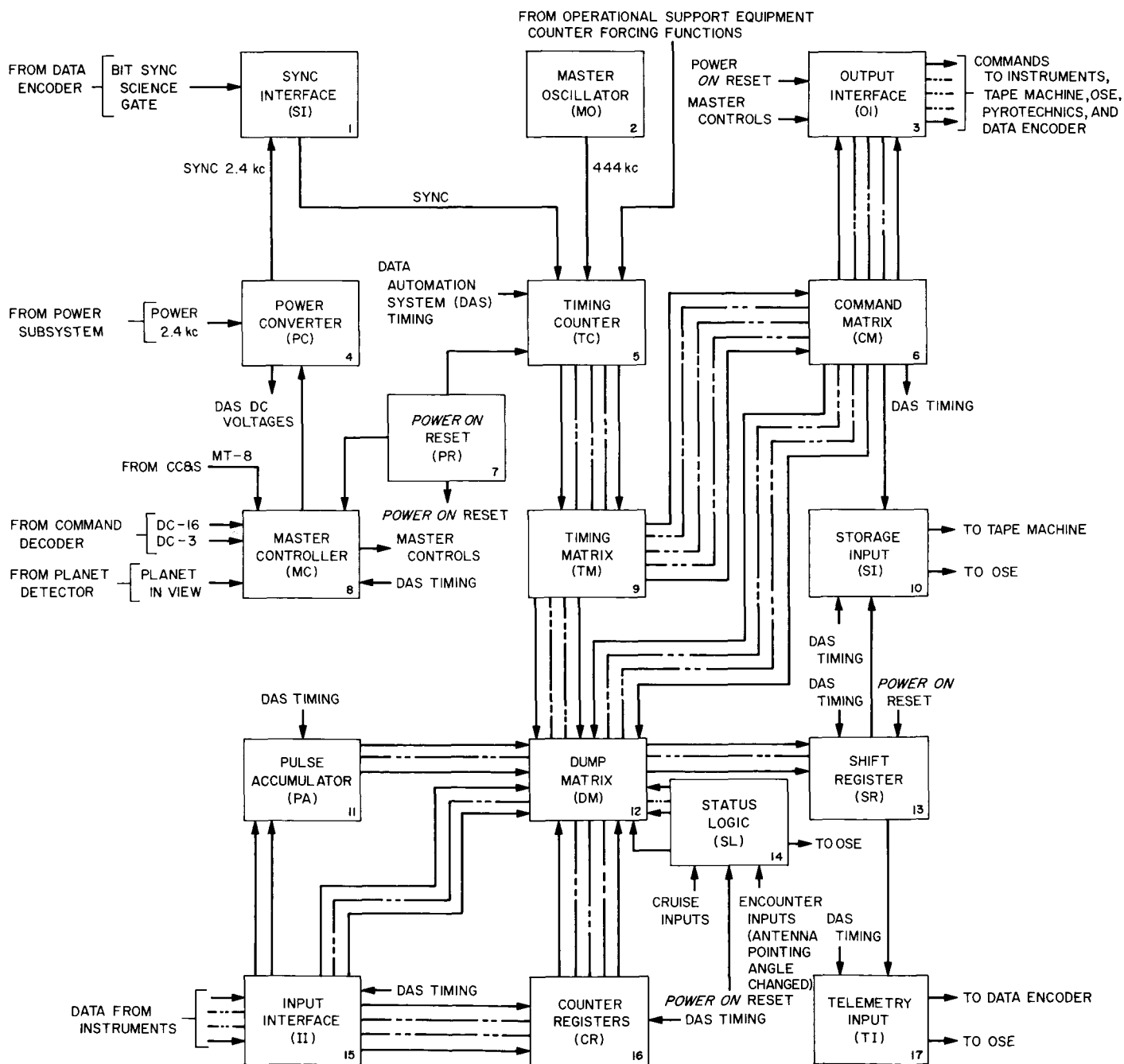


Fig 1. Science DAS block diagram, *Mariner Venus 67*

Because of the schedule and cost constraints, it was decided to concentrate effort on those tasks imposed by a new payload. It was decided to utilize, wherever possible, existing knowledge in industry on logic and circuit design and in packaging and fabrication techniques. For this reason, the design is proceeding using a planar layout of integrated circuits mounted on printed circuit boards. At the same time, the process development investigations were started to demonstrate that these techniques and the environmental test requirements for deep space flight are compatible.

The functional operation of the DAS, to produce the data formats during the encounter sequence as shown, may be understood by reference to Fig. 1. Data from the instruments flows through an input interface (15) directly or via counter registers (16) or a pulse accumulator (11) to a dump matrix (12). The dump matrix is merely a switching device to send the data into the shift registers (13) where it may be transferred to the telemetry input (17) for transfer to the data encoder and subsequent transmission to the Earth or into a storage input (10) for storage in a tape recorder and later transmission to the Earth. All of these functions are controlled by the timing and command portion of the DAS, which has several distinct features. A clock and timing function (2), (5), (9) generates sequences which command the instruments to read out, format the data, and send it to its destination. The master controller receives ground commands from a command decoder or spacecraft command from the CC&S and planet sensor to initiate various functions. Bit sync from the data encoder is fed to the timing system and ensures synchronization with the telemetry input (17) and the data encoder.

Design, fabrication and testing of the *Mariner Venus 67* Science DAS is the subject of a contract with the Guidance and Controls Systems Division of Litton Systems, Inc.

B. *Mariner Venus 67* Data Automation System Format

The data automation system (DAS) format for the *Mariner Venus 67* mission has been established. This article describes the sequence in which the various instruments will be read out and the information transmitted to Earth. The particular format chosen represents

the best compromise for a number of instruments where readings equally spaced in time are necessary.

One frame of the DAS format is represented by Fig. 2. It consists of 42 words, each 10 bits in length, giving 420 bits/frame. In general, each word represents a reading from one instrument. The abbreviations are interpreted as follows:

PN	Pseudonoise sequence
PL	Plasma probe
M	Magnetometer (X, Y, and Z axes)
TRA	Trapped radiation analog
TRD	Trapped radiation digital
TRH	Trapped radiation high
TRL	Trapped radiation low
UV	Ultraviolet photometer (A, B, and C Detectors)
DFD	Dual-frequency digital
DFA	Dual-frequency analog
FCH	Frame count high
FCL	Frame count low

The letters above the various words indicate the registers (U through Z) in which the data are stored until read out by the DAS. The arrowheads below the beginning of the various words indicate the timing of the *read* and *control* functions of the DAS. For instance, at the beginning of Word 7, all three axes of the magnetometer are read simultaneously into registers X, Y, and Z. These registers are then read out sequentially in Words 7, 8, and 9. The plasma probe is stepped through its sequence of voltages by signals generated at the beginning of Words 2, 9, 16, etc.

In the cruise phase of the mission the first 28 words will be science, and the last 14 will be engineering measurements. At encounter the 42 words will occur as indicated.

All DAS functions will be synchronized to the telemetry bit rate. For the first 30 days of the mission, the telemetry bit rate will be 33½ bits/sec; thereafter the rate will be 8½ bits/sec. At the high data rate, one complete frame will be transmitted every 12.6 sec; at the low rate it will take 50.4 sec.

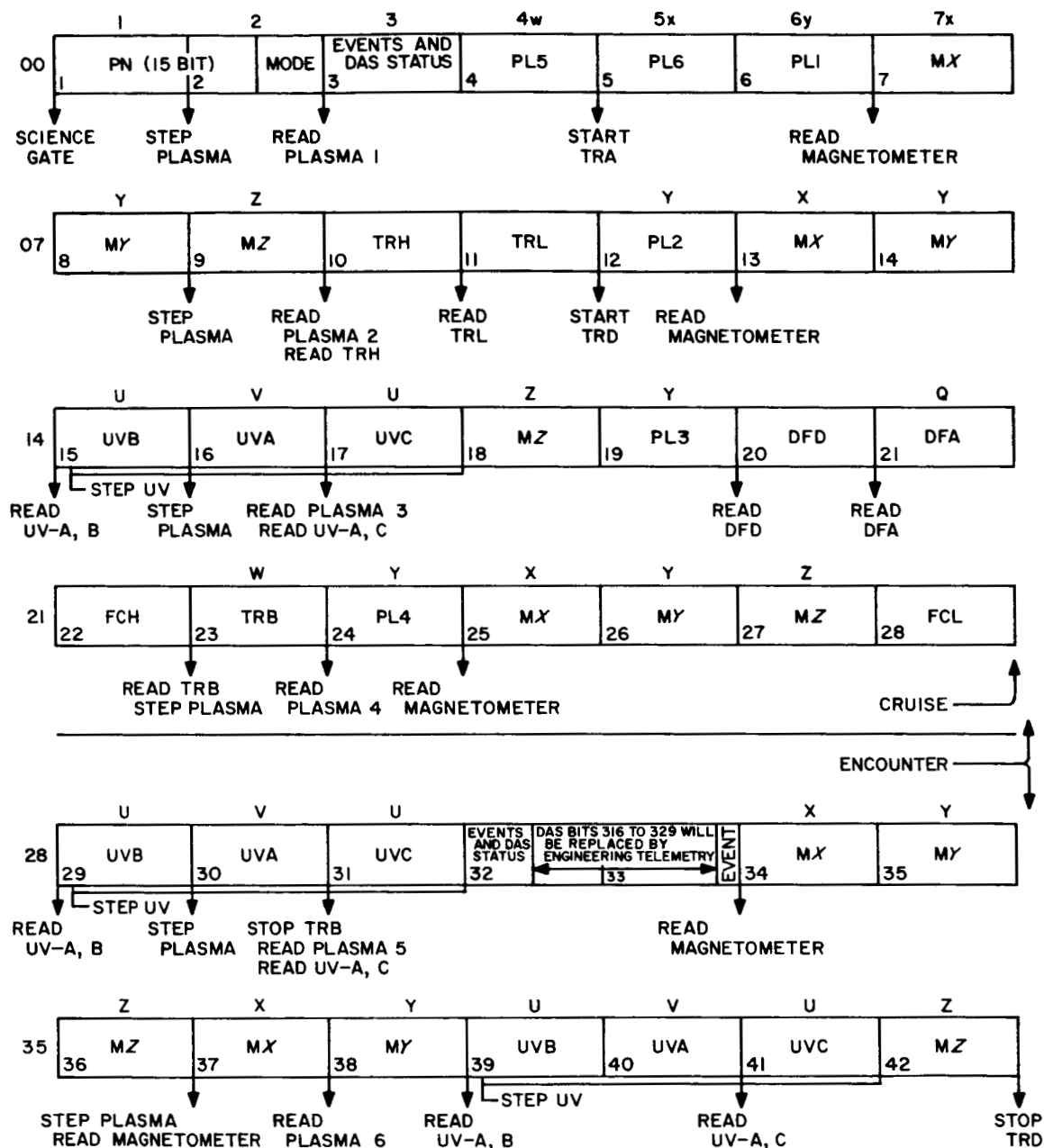


Fig. 2. Real-time DAS format

XI. Lunar and Planetary Sciences

A. Mariner Venus 67 Dual-Frequency Radio Occultation Experiment

a. Introduction. The dual-frequency radio occultation experiment was proposed by members of the Stanford University Center for Radar Astronomy. NASA announced the acceptance March 3, 1966, with Dr. V. R. Eshleman as principal investigator. Co-investigators are: Dr. G. Fjeldbo, H. T. Howard, R. L. Leadabrand, R. A. Long, Dr. B. B. Lusignan, and Dr. A. M. Peterson.

The receiver will be designed and built by the Stanford Research Institute, with TRW Systems as a subcontractor. JPL personnel assigned are: F. T. Barath, cognizant scientist, and D. P. Martin, cognizant engineer. The experiment description is a summary from Ref. 1.

b. Summary. The experiment will measure interplanetary electron densities and the atmosphere and ionosphere characteristics of Venus during the encounter. Frequencies of 49.8 and 423.3 MHz will be transmitted by the 150-ft antenna at Stanford University to the spacecraft dual-frequency receiver (DFR). The receiver will measure the dispersive doppler frequencies, differential group path, signal amplitudes, and signal frequencies. The flight data will be returned through the spacecraft telemetry

system. The encounter data will be tape recorded and transmitted back after encounter.

c. Experiment description. During the cruise from Earth to Venus, the instrument will provide a means of deducing the interplanetary electron density. The phase of a wave passing through an ionized medium is advanced so the ray path is bent by an amount inversely proportional to the frequency and directly proportional to the integrated electron density. The modulation envelope is delayed by the same amount. A sufficiently high frequency is relatively unaffected by the amount of ionization in interplanetary space. Thus the relative phase of the modulation envelope provides a measure of the integrated electron density and the rate of change of phase of one carrier, with respect to the other, is a measure of the rate of change of integrated electron density.

The experiment uses two high-power ground transmitters and a 150-ft parabolic antenna to transmit phase-modulated signals to the receiver on the spacecraft. Presently available, and in use on the *Pioneer* Program, are a 30-kw average power transmitter at 423.3 MHz and a 300-kw average power transmitter at 49.8 MHz. The antenna and transmitters are located at the Stanford Center for Radar Astronomy. Both carriers are phase modulated with an index of 0.9 so that the sum of the first-order sideband power equals the carrier power. The modulation frequency is either 7692 or 8692 Hz. The two modulation frequencies allow ambiguities up to 2800 deg of phase

shift to be resolved. The carrier frequencies have a long-term stability of five parts in 10^{10} . Small adjustments in frequency to reduce the receiver loop stress are possible.

The dual-frequency receiver (DFR) is described in the following sections. Its performance characteristics are presented now to complete the experiment description. The accuracy of the group path measurement determines the total integrated electron density error. Thus a ± 6 -deg phase error at 8692 Hz results in $\pm 4.3 \times 10^{16}$ electrons/m² error in group path. The maximum unambiguous integrated electron density is 1.7×10^{19} electrons/m² for eight cycles of 8692 Hz.

The phase path change is obtained by counting the normalized frequency difference between the carriers. The counter, for a 1-min sampling interval, has an error of ± 1 cycle of Δf which corresponds to a rate of change of integrated electron density error of $\pm 6 \times 10^{12}$ electrons/m²-sec. The maximum rate of change of integrated electron density without ambiguity, $\pm 3.2 \times 10^{15}$ electrons/m²-sec, is determined by the maximum frequency difference of 8.5 cycles.

The receiver is calibrated every 28 hr during the interplanetary cruise. A *calibrate* command from the data automation subsystem disconnects the 49.8-MHz channel and connects both IF inputs to the 423.3-MHz channel. This establishes the output of the modulation phase detector for zero phase shift relative to the 423.3-MHz channel.

During encounter the same measurements are made. If Venus has an ionosphere, the electron density will be much greater. If the trajectory is such that the craft passes behind the planet as viewed from the Earth, the radio ray path from transmitter to receiver will pass tangentially through the atmosphere and be occulted at the limb. Perturbations imposed on the radio waves by the planetary atmosphere provide a sensitive measure of atmospheric parameters. The basic quantity in such an experiment is the profile in height of the refractive index of the atmosphere. Both the neutral and the ionized regions of the atmosphere will, in general, contribute to this profile. Ref. 1 discusses a similar experiment in greater detail.

As an approximation to the radio phase effect, assume straight-line propagation through the ionosphere. This simplification gives a first approximation ϕ_1 to the phase path increase

$$\phi_1(\rho) = \frac{1}{\lambda} \int_{-\infty}^{+\infty} (\mu - 1) dz \quad (1)$$

where λ is the free space wavelength, μ is the refractive index in the ionosphere, ρ is the radius of closest approach, and z is the distance along the phase path.

The magnetoionic theory relates μ to the electron density N and the radio frequency f by:

$$\mu = 1 - (40.3/f^2) N \quad (2)$$

where it is assumed that the radio frequency is much larger than the maximum plasma-, collision-, and gyro-frequencies of the ionosphere.

Thus

$$\phi_1(\rho) = -40.3 I(\rho) \text{ cf cycles} \quad (3)$$

where c is the free-space phase velocity, and $I(\rho)$ is the electron content along the straight-line approximation to the propagation path. The function $I(\rho)$ is given by

$$I(\rho) = \int_{-\infty}^{+\infty} N dz \text{ elec/m}^2 \quad (4)$$

which is the integrated electron density.

The electron density profile can be determined from the radio occultation measurements in two steps:

First, we can determine the straight-line phase path $\phi_1(\rho)$, or the electron content profile $I(\rho)$, from a measurement of the phase or amplitude variations that occur during immersion and emersion.

Second, we can use the electron content profile to calculate the electron density profile, assuming that the ionosphere can be considered spherically symmetrical in those regions probed by the radio signals.

The radio waves are also refracted by the lower neutral atmosphere and diffracted at the planetary limb. These effects provide a sensitive measure of scale height and density in the neutral atmosphere, since the experiment provides separation of dispersive ionospheric refraction effects from the nondispersive effects of the neutral atmosphere.

In order to also illustrate the advantage of using two frequencies in the determination of the refractive index profile of the lower neutral atmosphere it will, in the following, be assumed that $\phi_1(\rho)$ has been calculated from

measurements at two frequencies f and mf . Taking into account the effect of both the ionized and the neutral part of the atmosphere, rewrite Eq. (1) in the following form:

$$\phi_1(\rho, f) = \frac{1}{\lambda} \int_{-\infty}^{+\infty} (\mu_n - 1) dz - \frac{40.3}{cf} \int_{-\infty}^{+\infty} N dz \quad (5)$$

where $\phi_1(\rho f)$ denotes the straight-line phase path at frequency f , λ the free space wavelength corresponding to the frequency f , and μ_n the refractive index profile of the neutral atmosphere. Similarly, write for the straight-line phase path at frequency mf

$$\phi_1(\rho, mf) = \frac{m}{\lambda} \int_{-\infty}^{+\infty} (\mu_n - 1) dz - \frac{40.3}{cfm} \int_{-\infty}^{+\infty} N dz \quad (6)$$

Thus

$$\frac{1}{\lambda} \int_{-\infty}^{+\infty} (\mu_n - 1) dz = \frac{m\phi_1(\rho, mf) - \phi_1(\rho, f)}{m^2 - 1} \quad (7)$$

from which the vertical refractive index profile of the lower neutral atmosphere can be determined. Eq. (7) shows that it is not necessary to assume a spherically symmetric ionosphere in order to determine the refractive index profile of the neutral atmosphere, when two frequencies are used in the occultation experiment. This result is important when very large ionospheric effects might otherwise mask the effect of a neutral atmosphere of low density.

d. Dual-frequency receiver description. The receiver will be supplied to JPL by Stanford University through subcontracts to Stanford Research Institute and TRW Systems. Fig. 1 is a simplified block diagram of the

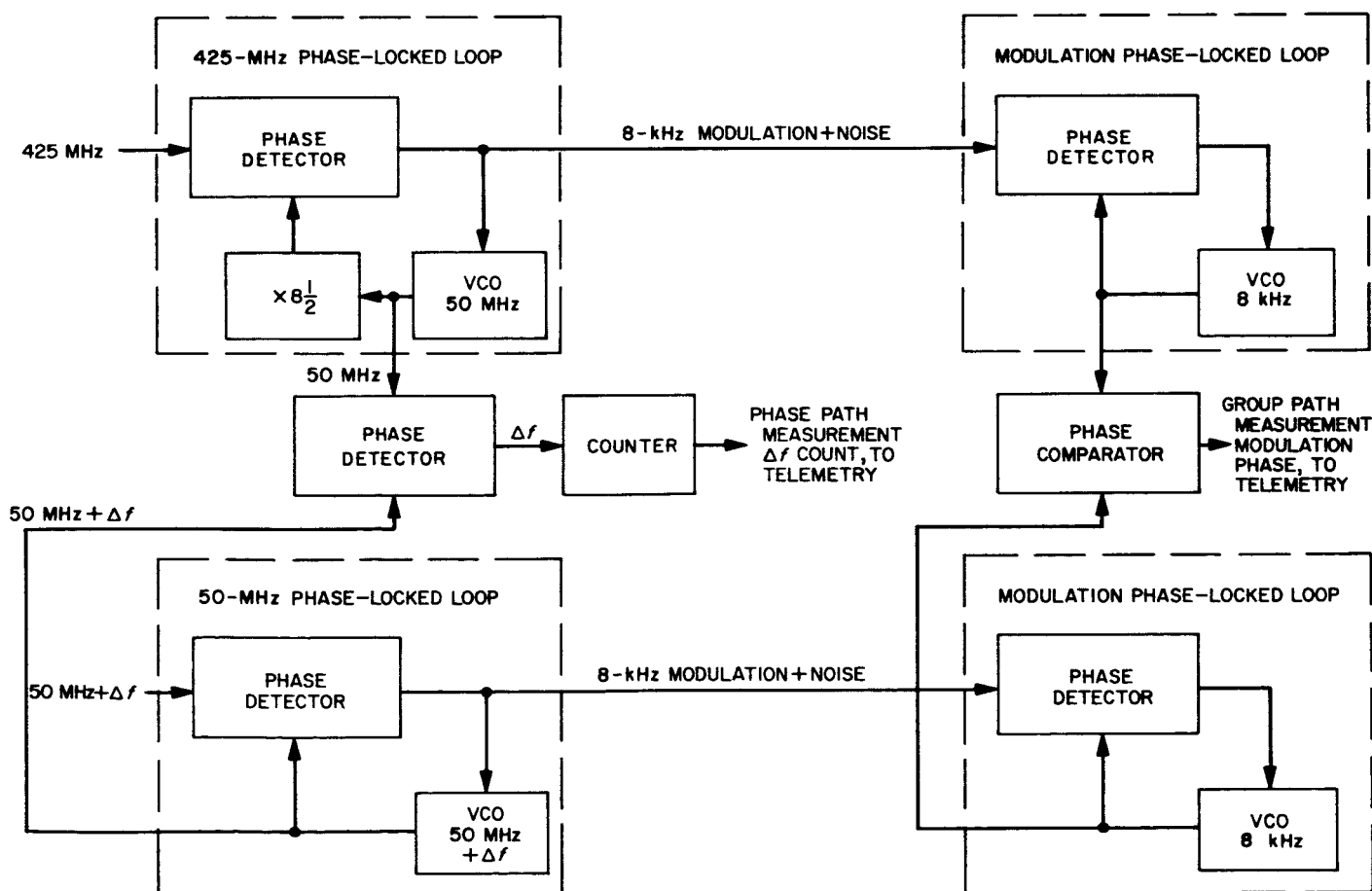


Fig. 1. Simplified block diagram of receiver

receiver. Two phase-locked loops enable the carriers to be filtered in a 10- to 20-cycle noise bandwidth. The differential phase path change is detected and stored in a 2^{10} binary counter. The modulation on each carrier (group path measurement) is demodulated by another pair of phase-locked loops and read out through a subcommutator. The actual implementation is slightly different from the simplified block diagram.

The receiver system noise temperature, referred to the antenna terminals, is 8300°K for the 49.8-MHz input and 1500°K for the 423.3-MHz input. These temperatures include the effects of cosmic noise, transmission line loss, and image response. The detailed calculations are presented in Ref. 2. The IF noise bandwidth of 45 kHz is determined by a crystal filter. The receiver threshold sensitivity is -129 dbm for 49.8 MHz and -136 dbm for the 423.3-MHz channel. Threshold sensitivity is defined as the power which gives a loss of 1 cycle in 10 hr.

The receiver depends on the data automation subsystem for pulses to initiate: digital data readout, calibration, reset, subcommutation, and subcommutated data readout. The subcommutated analog data are converted to pulse width data in the receiver and read out as DAS Word 21. (Every other frame from the subcommutator will be modulation phase while the intervening frames will be sequentially 49.8 MHz carrier amplitude, VCO loop stress, 423.3 MHz carrier amplitude, and VCO 2 loop stress.)

The receiver requires less than 2 w of power from the spacecraft 2400-cycle supply of $\pm 50\text{ v}$. The receiver weighs 5 lb, excluding the antennas. The lower frequency antenna is obtained by shunt-feeding two of the solar panel frames. The 423.3-MHz antenna is a quarter-wave stub with two reflectors to increase the gain. It is mounted on the end of one solar panel. The receiver is constructed on two subchassis which amount in the scientific equipment case.

References

1. Fjeldbo, G., Eshleman, V. R., Garriott, O. K., and Smith, F. L., III, "The Two-Frequency Bistatic Radar-Occultation Method for the Study of Planetary Ionospheres," *Journal of Geophysical Research*, Vol. 70, No. 15, August 1, 1965.
2. Koehler, R. L., "A Phase-Locked Dual Channel Spacecraft Receiver for Phase and Group Path Measurements," Stanford University Radioscience Laboratory Report SEL-65-007, February 1965.

XII. *Mariner* Space Sciences

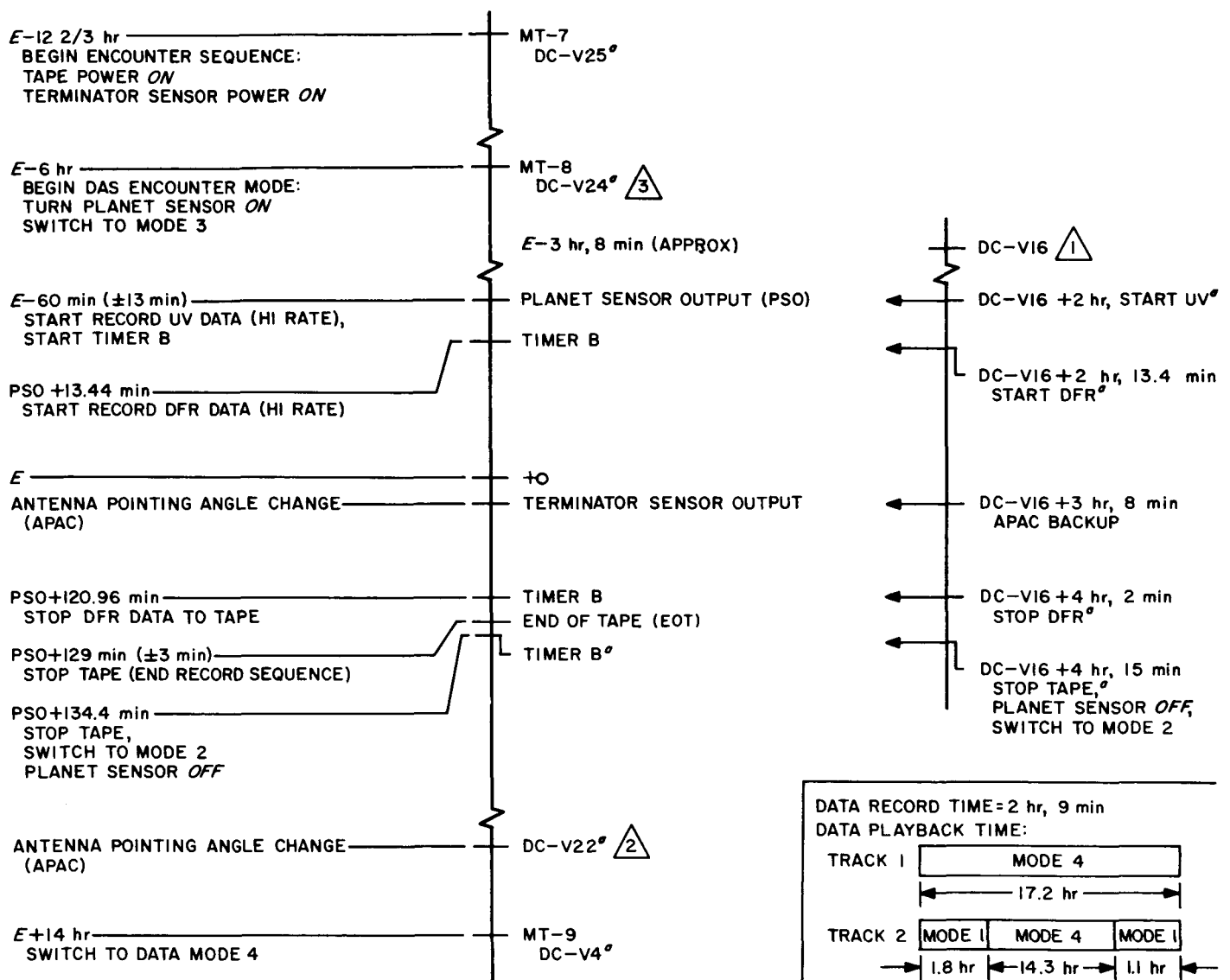
A. *Mariner* Venus 67 Encounter Sequence

From a scientific standpoint, the most crucial phase of the *Mariner* Venus 67 mission is the encounter. Two Data Automation System (DAS) timers, designated A and B, are employed in a redundant fashion to assure the proper sequence of events at the appropriate times. In Fig. 1, the sequence of events initiated by Timer A is indicated on the right-hand vertical line. The same series of events appear on the left-hand line, as initiated by Timer B. Timer A is started by ground command (DC-V16) approximately 188 min prior to closest approach (E), while Timer B is started by an output from the planet sensor, which should occur at approximately $E - 60$ min.

As the spacecraft approaches the planet, the data encoder will be operating in Mode 2, i.e., of the information coming from the spacecraft, $\frac{2}{3}$ will be science and $\frac{1}{3}$ will be engineering data. At $E - 12\frac{1}{2}$ hr the CC&S master timer (MT-7) will initiate the encounter sequence by turning on power to the tape recorder and the terminator sensor. A ground backup command (DC-V25) can

ensure this action. In the ensuing $6\frac{1}{2}$ hr, the effects of event MT-7 will be reflected in the engineering data. At $E - 6$ hr, another signal from the master timer (MT-8) will cause the DAS to enable timer B, apply power to the planet sensor and switch the data encoder to Mode 3. A ground command (DC-V24) can ensure these actions. In Mode 3, almost all of the data transmitted are science.

Approximately 60 min before closest approach the prevailing timer (A or B, whichever provides the first output) will control the indicated series of events. The data will be simultaneously tape recorded and transmitted in real-time, but occultation will prevent reception of the real-time data for approximately 25 min, beginning shortly after closest approach. After a total recording time of 129 min, the tape recorder will stop and 5 min later the prevailing timer will end the encounter sequence and return the data encoder to Mode 2. When the spacecraft leaves occultation, a ground command (DC-V22) may be used to change the antenna pointing angle if this did not occur at the appropriate time. At $E + 14$ hr a signal from the master timer (MT-9) will initiate the tape recorder playback. A ground command (DC-V4) is provided as backup for this event.



°BACKUP

- ¹ DC-VI6 TOGGLES (*ON/OFF*) DAS CLOCK TO ISSUE BACKUP COMMANDS DURING ENCOUNTER SEQUENCE. COMMAND TRANSMITTED SO THAT TIMER A BACKS UP TERMINATOR SENSOR. OTHER BACKUPS OCCUR ACCORDINGLY
- ² DC-V22, IF REQUIRED, WILL BE TRANSMITTED AS SOON AS POSSIBLE AFTER ENCOUNTER
- ³ DC-V24 ALSO TOGGLES (*ON/OFF*) TIMER B INHIBIT

Fig. 1. Encounter sequence

SUPPORTING ACTIVITIES

XIII. Environmental Test Facilities

A. Surveyor and Mariner Venus 67 Solar Panel Thermal Radiation Fixture

A new solar panel thermal-vacuum test fixture has been developed to satisfy higher temperature (170°C) test requirements for solar panel testing in the JPL 7-ft vacuum chamber. In addition to the higher temperature capability, the fixture provides closer temperature control (10°F) than has been possible with previous techniques.

The fixture consists of an aluminum frame supported from the 7- × 14-ft vacuum chamber door (Fig. 1). Thirty

2500-w, 440-v, 3-phase quartz lamps and semicylindrical reflectors are mounted on the rack 10 in. below the solar panel. Two 440-v, 30-amp, 3-phase variacs provide thermal control. The infrared lamp bank test fixture used for the *Mariner IV* program required a shield to protect the solar panels being tested from lamp explosion hazards. The present thermal radiation fixture utilizes quartz lamps and was designed to eliminate such hazard.

To date, the fixture has been subjected to 200 hr of evaluation tests which included 120 hr of preproduction prototype *Mariner Venus 67* solar panel testing in the vacuum chamber.

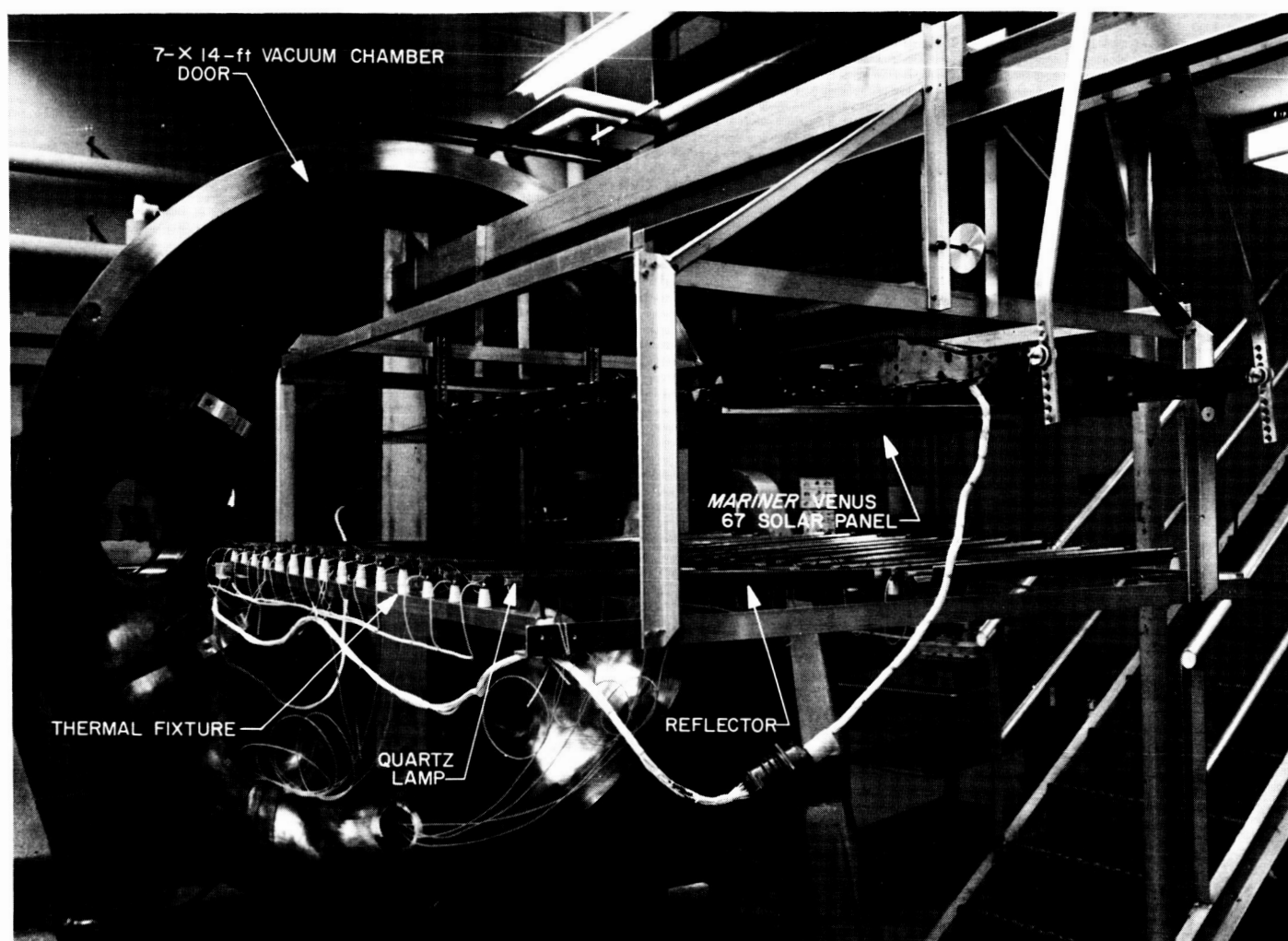


Fig. 1. Mariner Venus 67 solar panel thermal-vacuum test fixture